Exp Brain Res (1997) 117:219–241

RESEARCH ARTICLE

Lionel G. Nowak · Andrew C. James · Jean Bullier

Corticocortical connections between visual areas 17 and 18a of the rat studied in vitro: spatial and temporal organisation of functional synaptic responses

Received: 28 February 1996 / Accepted: 31 January 1997

Abstract Much is known about the anatomy of corticocortical connections, yet little is known concerning their physiology. In order to have access to the synaptic and temporal aspects of the activity elicited through corticocortical connections, we developed an in vitro approach on slices of rat visual cortex. We used extracellular recordings of field potentials combined with electrical stimulation to localise regions of areas 17 and 18a that are connected. We found that corticocortical connections between areas 17 and 18a can be preserved in 500 μm thick slices, with a focus of activity separated from the stimulating electrode by 1.5 mm to more than 3 mm. The potentials elicited in one area after stimulation of its neighbour displayed fast events, corresponding to action potentials, and slow events, corresponding to synaptic potentials. Intracellular recordings showed that the earliest synaptic responses consisted of monosynaptic excitatory potentials. Measurement of response latency showed that axons involved in both feedforward and feedback corticocortical connections are slowly conducting (0.3–0.8 m/s). Conduction velocity for antidromically activated cells was not significantly different for the two sets of connections. In an attempt to establish the spatial organisation of functional synaptic inputs, field potential recordings were performed in the different cortical layers and used to establish current source density (CSD) graphs along the depth axis. The CSD maps obtained were found to be somewhat variable from one case to another. It is suggested that this variability results from the use of electrical stimulation, which activates axons that are both afferent and efferent to a given cortical area. The field potentials are therefore likely to contain responses that correspond to the activity mediated by the intrinsic collaterals mixed in variable amount with responses produced by corticocortical synapses. With this restriction in mind, it is suggested that, after stimulation of the supragranular layers, the functional synaptic inputs of feedforward connections are concentrated in layer 4 and the bottom of layer 3, while those of feedback axons involve mainly the upper part of the supragranular layers. The intrinsic collaterals of the neurones participating in corticocortical connections seem also to provide the bulk of their inputs to the upper part of the supragranular layers. The laminar pattern of activity obtained after infragranular layer stimulation was comparable to that obtained after supragranular layer stimulation, except for the addition of a supplementary region of activated synapses in the infragranular layers.

Key words Visual cortex · Slice · Field potentials · Current source density · Latency

L.G. Nowak[1] · A.C. James[2] · J. Bullier (✉)
INSERM Unité 371, Cerveau et Vision,
18, avenue du Doyen Lépine, F-69675 Bron Cedex, France

Present addresses:
[1] Section of Neurobiology, Yale University School of Medicine, C303 Sterling Hall of Medicine, 333 Cedar Street, New Haven, CT 06510, USA
[2] Developmental Neurobiology, RSBS ANU, GPO Box 475, Canberra ACT 2601, Australia

Introduction

The visual cortex of mammals is composed of a number of areas, which contain a more or less complete representation of the contralateral visual hemifield. In the rodent, area 17 appears to be the main recipient of the visual inputs relayed through the lateral geniculate nucleus (Ribak and Peters 1975; Hughes 1977; Dürsteler et al. 1979; Spatz et al. 1991). Two other cytoarchitectonic areas of the occipital cortex, referred to as area 18a and area 18b (after Krieg 1946a, b), have been associated with vision. Area 18b lies medial to area 17 and area 18a lateral and rostral to 17. Within area 18b and 18a (and area 7 of Krieg 1946a), the existence of about ten functional visual areas has been demonstrated by mapping studies (Montero 1973; Montero et al. 1973a; Thomas and Espinoza 1987), labelling of ipsilateral corticocortical connections (Montero et al. 1973b; Olavarria and Montero 1981, 1984; Montero 1993; Coogan and Burkhalter 1993), labelling of callosal connections (Cusick and

Lund 1981; Olavarria and Montero 1984; Thomas and Espinoza 1987; Coogan and Burkhalter 1993) and voltage-sensitive dye studies (Orbach and Van Essen 1993).

The different visual cortical areas tend to be reciprocally connected. Initially in the monkey, it has been shown that different types of corticocortical connections can be distinguished on the basis of the laminar distribution of parent neurones and terminal axonal arborisation. Neurones that provide *feedforward* inputs are mainly located in the supragranular layers, and their axonal terminals are found at the level of layer 4 and the bottom of layer 3 (Rockland and Pandya 1979; Maunsell and Van Essen 1983). In contrast, *feedback* connections arise mainly from infragranular layers neurones, although a substantial proportion of supragranular layer neurones participate in these connections when the two areas are near each other (Rockland and Pandya 1979; Maunsell and Van Essen 1983; Kennedy and Bullier 1985). Terminals of feedback connections are found throughout the different cortical layers, except in layer 4, with a predominance in layer 1 (Tigges et al. 1977; Rockland and Pandya 1979; Lund et al. 1981; Maunsell and Van Essen 1983; Rockland and Virga 1989; Rockland et al. 1994).

The anatomical organisation of rat visual cortex does not appear as ordered as that of the primates. Area 17 neurones sending feedforward connections are present not only in the supragranular layers, but also in substantial numbers in layers 4, 5 and 6 (Dürsteler et al. 1979; Olavarria and Montero 1981; Miller and Vogt 1984; Coogan and Burkhalter 1988; Burkhalter and Charles 1990; Johnston and Burkhalter 1994). The projection layers of feedforward axons are a matter of debate. Using anatomical techniques, some authors found terminals in supragranular layers with little involvement of layer 4 (Montero et al. 1973b). Others observed a denser labelling in layer 4 than in other layers (Olavarria and Montero 1981). One study reported labelling in all layers *excluding* layer 4 (Miller and Vogt 1984*)*, whereas a recent report reached the conclusion that all layers receive feedforward inputs (Coogan and Burkhalter 1993). A possible explanation for these discrepancies is the recent observation that, in the cat (Henry et al. 1991) and the rat (Coogan and Burkhalter 1993), anterograde tracer injections restricted to the upper layers tend to label axon terminals mainly in the upper layers, whereas injections placed deeper in cortex lead, in addition, to a substantial amount of labelling in the infragranular layers.

The neurones providing the feedback inputs from extrastriate cortex to area 17 are found, like parent neurones of feedforward connections, in all cortical layers (Dürsteler et al. 1979; Olavarria and Montero 1981; Miller and Vogt 1984; Dreher et al. 1985; Johnson and Burkhalter 1994). Terminals of feedback axons, as in other mammals, are not observed in layer 4 but are present in all the other layers, with a predominance in layer 1 (Miller and Vogt 1984; Johnson and Burkhalter 1992; Coogan and Burkhalter 1993).

Much of the research on corticocortical connections has concentrated on their anatomical organisation. Less is known, however, concerning the physiological functions they participate in. In order to gain a more complete understanding of the functions of corticocortical connections, it is necessary to have access to the temporal and synaptic aspects of the responses they elicit. For that purpose, we developed an in vitro approach on slices of rat visual cortex. An in vitro study of corticocortical connections requires that they are preserved in slices, and that they can be identified easily by electrophysiological methods. For this identification, we relied on electrical stimulation and recording of field potentials to map the visual cortex in order to identify interconnected regions in two cortical areas (areas 17 and 18a).

We were mostly interested in the synaptic physiology of corticocortical connections. Field potentials provide information about the latency and strength of the synaptic responses elicited by electrical stimulation. When combined with current source density (CSD) analysis, they also give access to the location of the activated synapses (Haberly and Sheperd 1973; Freeman and Nicholson 1975; Nicholson and Freeman 1975; Mitzdorf and Singer 1978, 1979; Mitzdorf 1985). We therefore attempted to study the pattern of CSD produced in the different cortical layers to determine the *functional* organisation of corticocortical synaptology. This functional organisation may differ from that inferred from labelling studies, which do not give indication on the strength of synaptic inputs present in a given cortical layer. Both feedforward and feedback connections were studied this way. Because terminals of projections from upper and lower layers neurones seem to be somewhat segregated in the depth of the target area (Henry et al. 1991; Coogan and Burkhalter 1993), we also compared the field potentials and CSD maps obtained after supra- and infragranular layer stimulation. Some aspects of the results obtained using field potential recordings were further studied using intracellular and extracellular single unit recordings.

Materials and methods

Brain slice preparation

The brain slice preparation has been described in detail in another paper (Nowak and Bullier 1996). Under deep halothane anaesthesia, male or female, Wistar or Sprague Dawley rats (150–300 g) were perfused through the heart with a modified Artificial Cerebro-Spinal Fluid (mACSF) at a flow rate of 10 ml/min. The composition of the mACSF, intended to provide a protection against ischaemia, was (in mM): NaCl 91.7; $NaHCO_3$ 24; NaH_2PO_4 1.2; KCl 3; $MgCl_2$ 19; $MgSO_4$ 1; D-glucose 25. It was oxygenated for 1 h before the beginning of the surgery with a mixture of 95% O_2 and 5% CO_2, and cooled to 3–4°C.

After removal of the skull, the whole brain was removed and 500 μm thick, coronal slices were prepared with a vibratome (Oxford). The slices were thereafter stored at room temperature for at least 1 h in a chamber filled with 800 ml of a standard Artificial Cerebro-Spinal Fluid (ACSF) of the following composition (in mM): NaCl 126; $NaHCO_3$ 24; NaH_2PO_4 1.2; KCl 3; $CaCl_2$ 2.5; $MgSO_4$ 1; D-glucose 10. The chamber was bubbled with a mixture of 95% O_2 and 5% CO_2 (pH 7.4). Recordings were performed in a submersion type chamber where the temperature was

33–34°C. The standard ACSF was gravity-fed at a flow rate of 6–8 ml/min.

Recording and stimulation

Intracellular recordings were made with micropipettes pulled on a BB-CH puller (Mecanex, Geneva) from 1.2 mm OD capillaries with internal microfibre (Clark Electromedical Instruments). Micropipettes were filled with 3 M potassium acetate (DC resistance 80–120 MΩ). Extracellular recordings of field potentials were made with glass micropipettes filled with 1 M NaCl (DC resistance 1–5 MΩ). For precise visualisation of their placement, the tips were painted black with permanent ink.

Intracellular and field potentials were amplified on an amplifier (Biologic VF 180) containing an active bridge circuit as well as capacity and resistance compensations, followed by a Neurolog device for further amplification and filtering. For field potentials, a high frequency cut-off of 1 kHz was used, while the low frequencies were not filtered.

Extracellular recordings of single units were made with tungsten-in-glass microelectrodes (Merrill and Ainsworth 1972) with 15–25 μm exposed tips and plated with platinum black (impedance <0.5 MΩ at 1000 Hz). Signals were amplified and filtered with the Neurolog recording system.

Cathodal monopolar electrical stimulation was applied at a frequency of 0.5 or 0.3 Hz (pulse duration 0.2 ms) through a stimulation isolation unit (Neurolog). For the field potential studies, the stimulation intensity was 50 μA in all cases, except when we studied the relationship between stimulus intensity and amplitude of the evoked potential (Fig. 3). According to our measurements of stimulating current spread (Nowak and Bullier 1996), an intensity of 50 μA should activate axons in a sphere 40–150 μm in diameter. Stimulating electrodes were tungsten-in-glass microelectrodes for which the glass was generally removed over a length of 100–200 μm from the tip. For a subset of cases of intracellular recording and for a subset of extracellular recording of antidromic action potentials, the glass was removed over a length of 15–25 μm only.

Signals were visualised on line on a Philips oscilloscope (PM 3335), from which hard copies were printed using an X-Y plotter (Hewlett Packard 7470A). When signals were averaged (on line), an averaging oscilloscope (Hewlett Packard 54501A) was used, from which hard copies were printed on a Hewlett Packard (Think Jet) printer.

Current source density analysis

Field potentials were averaged over 30–50 stimulus repetitions. The corresponding plots were enlarged and sampled using a digitising tablet. The high-frequency noise was filtered out in this process. The stimulation artefact per se was not sampled, but the shift of potential it induced was sampled since part of it may overlap with potential changes of neuronal origin. The digitising tablet and the associated software transformed the traces in ASCII files. Files of voltage/time sequences were obtained with a sampling frequency around 500 points per 100 ms. These irregularly spaced time series were smoothed and interpolated using a thin-plate spline technique (see below) and then resampled at a uniform sampling interval of 0.2 ms.

Each *averaged waveform* was then digitally low-pass filtered to give the *filtered response*, using a Butterworth digital filter with a cut-off frequency of 2000 Hz. The filter coefficients were of order 4, and each waveform was filtered forwards and backwards in time, which gives a total filter order of 8 and zero phase distortion at all frequencies.

For each point in time, the waveforms were then interpolated over the *spatial* domain with a one-dimensional thin-plate spline (Wabha 1990). This gives at each time-point the curve that minimises a hybrid cost function consisting of the residual sum of squares between data values and fitted curve, plus a smoothing parameter (lambda) times the bending energy, defined as the square of the second derivative integrated over space. The parameter lambda adjusts the degree of smoothing of the interpolation: a value of zero gives the classical cubic spine interpolation, while in the limit for large lambda, the interpolation tends towards the least-squares regression line. In all the cases a small value of lambda (0.0001) has been used, that produced only a limited filtering in the spatial dimension.

Interpolated responses were calculated for a regular sequence of spatial locations at 5 times finer spatial resolution than the original data. For the lateral sequences of recording (Figs. 1, 2) and for depth sequences (Figs. 5–8), the interpolated field potentials are plotted as contours on the domain of time and space. Contour step size is indicated above or within the contour plot; the interior of the negative contours is shaded. The contour at zero is omitted to avoid excessive noisiness.

For recording sequences obtained over depth through the layers of the cortex (Figs. 5–8), the *current source density* (CSD) was estimated by the negative of the second differences over depth for the interpolated responses, divided by the square of the interpolating depth-step size (100 μm). This gives values in units of millivolts per square millimetre. Contour plots of estimated CSD are presented on the domain of time and space, in alignment with the contour plot of the corresponding field potential. CSD step size is indicated above the contour plot, the interior of the negative contours, corresponding to current sinks, is shaded, and the contour at zero value is omitted.

Criteria for identification of antidromic activation and latency measurements

The identification of antidromic action potentials in extracellular recordings relied on the following criteria: (a) The latency should not vary when the current intensity was 1.5 times the threshold current intensity. (b) The latency should not decrease by more than 10% when current intensity was raised from threshold to twice the threshold. (c) The refractory period should be lower than 3 ms. (d) The activation should be observed during high-frequency stimulation (100 Hz or more during 200 ms). The validity of these criteria for the identification of antidromic action potentials was confirmed in five cases for which recordings were performed in a medium where Ca^{2+} was replaced by 2 mM Mn^{2+}.

Antidromic action potentials were also recorded in two intracellularly recorded neurones and were identified by their constant latency, the absence of an underlying excitatory postsynaptic potential (EPSP) and the occurrence of initial segment spikes that could be evoked without soma-dendritic spikes.

For single units, the latency was measured between the beginning of the stimulation artefact and the foot of the action potential. The onset latencies of field potentials have been measured for the potentials presenting the largest amplitude in laminar profile analysis. If antidromic action potentials obscured the onset, the latency of the nearest potential was used. Only the cases with supragranular layer stimulation have been taken into account. With infragranular layer stimulation, there was a risk of activating not only the axons involved in corticocortical connections but also axons from other sources travelling in the lower part of the grey matter, such as bifurcating thalamocortical axons.

Histology

In the initial experiments, electrolytic lesions were made at the stimulation and recording sites of interest. In later experiments, reference points were placed by pressure ejection of alcian blue dissolved in ACSF through a broken glass micropipette. The ejection was made in the white matter, in order not to disturb the neurones at stimulation and recording sites. For the reconstruction of the different recording and stimulation positions with respect to the cortical layers and to the 17–18a border, the X-Y coordinates of the stimulating and recording positions, of the dye injection

sites, of the pial surface and of the white matter at different places were measured from the cursors of one of the micromanipulators. These cursors had a precision of 10 μm.

After the experiment, slices were placed in fixative (4% paraformaldehyde in phosphate buffer), then in a sucrose solution (10% then 30% in phosphate buffer). Sections 40 or 50 μm thick were made on a freezing microtome and stained with cresyl violet.

Statistics

Data are given as mean ± 1 standard error of the mean. The Mann-Whitney *U*-test was used for statistical comparisons.

Results

General

For convenience, experiments in which electrical stimulation was applied in area 17 and recordings obtained in area 18a will be termed 'feedforward' experiments, although the present results suggest that feedforward connections were not the only set of connections to be activated (see Discussion). With the same reservation, experiments for which stimulation was applied in area 18a and recordings obtained in area 17 will be termed 'feedback' experiments.

The data base includes intracellular recordings from 21 neurones recorded in the upper half of the cortex. The membrane properties have been measured for 18 of these neurones and were the following: the resting membrane potential (RMP) was –78.7 ± 2.1 mV. All action potentials were overshooting. When measured from rest, their amplitude averaged 106.6 ± 3.3 mV, and 75.6 ± 2.3 mV when measured from spike threshold. The input resistance and time constant, determined from injection of small negative current (–0.1 nA), were respectively 41.5 ± 5.0 MΩ and 7.9 ± 0.9 ms. The width of the action potentials measured at half height from threshold was 0.75 ± 0.08 ms. In all the cases, the rising phase of the action potential was shorter than the falling phase. In addition, all the cells presented an accommodative discharge in response to the injection of long lasting depolarising current. These features are those of 'regular spiking' cells (Connors et al. 1982; McCormick et al. 1985).

Localisation of the parts of area 17 and 18a that are interconnected

Corticocortical connections between areas 17 and 18a are organised in a retinotopic fashion (Montero 1993). It follows that low-intensity electrical stimulation applied at a given location in one area will activate only the region containing the terminals of the axons activated by the stimulation. We relied on this organisation to localise the interconnected regions of the two cortical areas. For that purpose, we recorded field potentials at increasing horizontal separations (i. e. along the medio-lateral axis) from the stimulating electrode.

The alteration in field potential shape and amplitude for increasing horizontal separations and its relationship to the border between the cortical areas is illustrated in Fig. 1 for a 'feedforward' experiment. Figure 1A shows a cresyl violet stain of the slice. The border between areas 17 and 18a is indicated by the arrow. It was identified by a decrease in cell density in layer 4 of area 18a compared with that of area 17.

The same slice is schematised in Fig. 1B. The electrical stimulation was applied in the supragranular layers of area 17 (cross on Fig. 1B). The field potentials were recorded in the supragranular layers of area 17 and 18a. Recording sites were spaced apart by 100 μm in the horizontal dimension (dots on Fig. 1B). The recordings were made 250 μm below the surface of the slice, as were all the other field potentials recorded in the present study. Recordings were located 400 μm from the pial surface, because preliminary experiments indicated that large 'feedforward' field potentials could be obtained at that distance. The smallest horizontal separation between the stimulating electrode and recording position was 0.6 mm, and the largest was 2.2 mm for the case illustrated.

Figure 1C shows the series of field potentials obtained at the different horizontal separations. Separations between 0.6 to 1.2 mm correspond to the field potentials obtained within area 17. The potentials obtained nearest to the stimulating electrode display a large negative component.

The traces obtained from 0.9 to 1.1 mm are characterised by a small positive component that precedes a slow negative component. The early positive potential is likely to correspond to a current source, i. e. to the current flowing out of the cells to match the inward current

Fig. 1A–D Modification of field potential shape and amplitude for increasing horizontal separations and its relationship to the border between cortical areas 17 and 18a in a 'feedforward' experiment. **A** Photomicrograph of a Nissl-stained section of the slice used for that experiment. The *open arrows* in white matter indicate the alcian blue labels used as landmarks. The *black arrow* indicates the border between areas 17 and 18a. **B** Schematic drawing of the same slice. The scale is not corrected for shrinkage. The cortical layers are indicated on the *right* (*w.m.* white matter). *Dotted line* is the border between cortical areas. The *cross* indicates the site of electrical stimulation. **C** Series of field potentials obtained for the different horizontal separations. The horizontal separation between stimulating electrode and recording positions is indicated on the *right* of the traces. **D** Spatio-temporal representation of the field potentials. The *grey areas* represent the negative potentials. Positive potentials were smaller than 0.015 mV and therefore do not appear. *Upper part* shows potentials after their resampling (see Materials and methods). The largest trace, which corresponds to the recording obtained at 0.6 mm horizontal separation, contains an inflexion not visible in **C**. This inflexion results from the sampling that did not take the stimulation artefact into account. *Lower part* Plot as a function of time and space of the field potentials. The plot shows two regions of negative potentials. One is confined to area 17, and corresponds to the intrinsic activity mediated through horizontal connections. The other is essentially contained within area 18a, with the largest amplitude at >1.5 mm (after interpolation) from the stimulating electrode

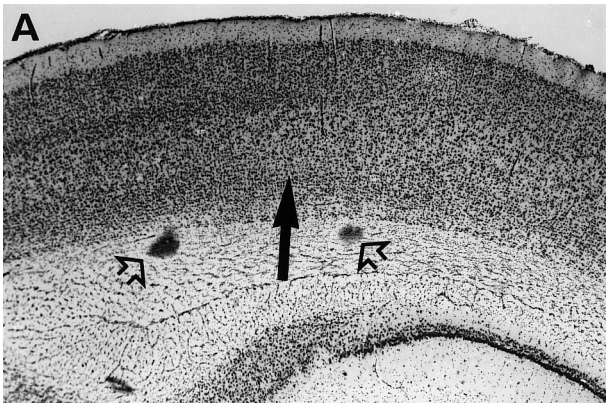
A

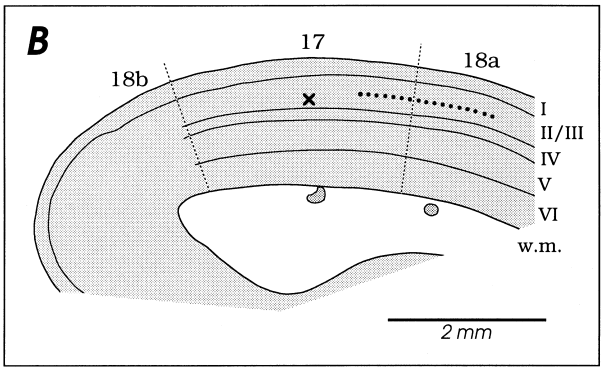
B
17
18a
18b
I
II/III
IV
V
VI
w.m.
2 mm

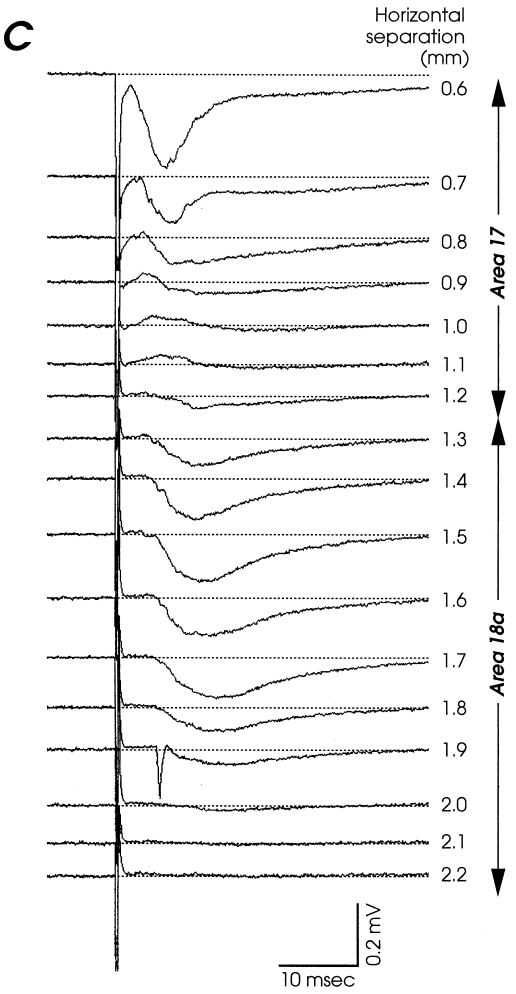
C
Horizontal separation (mm)
0.6
0.7
0.8
0.9
1.0
1.1
1.2
1.3
1.4
1.5
1.6
1.7
1.8
1.9
2.0
2.1
2.2
Area 17
Area 18a
0.2 mV
10 msec

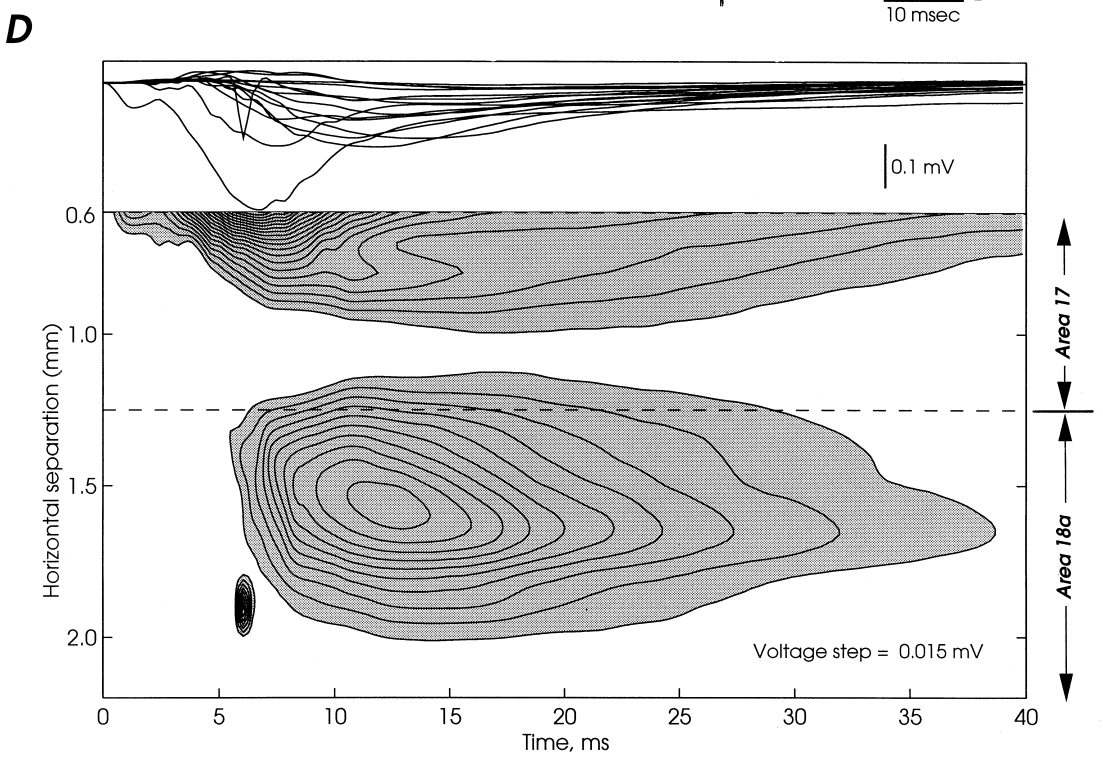
D
0.1 mV
0.6
1.0
1.5
2.0
Horizontal separation (mm)
Area 17
Area 18a
Voltage step = 0.015 mV
0
5
10
15
20
25
30
35
40
Time, ms

(sink) generated nearer the stimulating electrode. The slow negative potential following the positive one is characterised by its small amplitude and its long onset latency. It may correspond to polysynaptic activities transmitted through the intrinsic horizontal connections.

The potential obtained at 1.1 mm is nearly flat. Those obtained for larger separations show a negative component that increases in amplitude up to a maximum at 1.5 mm (within area 18a). These potentials are characterised by a constant and monophasic shape. Their negativity indicates their proximity to regions of depolarising responses. Their onset latency is about 5 ms. Their maximum amplitude is reached slowly, 5–7 ms after the onset, and their decay is monotonic, the baseline being reached about 40 ms after the stimulus. These features indicate a synaptic origin. The first negative trace was obtained at 1.2 mm, still within area 17. This is not incompatible with the presence of a current sink in area 18a, because field potentials spread in space away from the synapses that generate them.

The amplitudes of the potentials obtained at 1.8–2.0 mm decrease, indicating that the recording sites were moving away from the region of activated synapses (a large antidromic action potential is visible on the trace obtained at 1.9 mm). For the largest separations (2.1 and 2.2 mm), the potentials are flat. There is no region of positive potentials inserted between the negative and the flat potentials. Near the border of areas 17 and 18a there is also a lack of positive potentials with a time course comparable to the slow potentials recorded in area 18a. This suggests that, contrary to the potentials elicited within area 17, the current does not flow in the horizontal direction. Instead, most of the synaptic current generated in area 18a after stimulation in area 17 may flow in the vertical direction.

The contour map (Fig. 1D) summarises the pattern presented in the series of recordings of Fig. 1C. Large negative potentials are observed in area 17. Their amplitude decreases as the separation between recording and stimulating sites increases. Near the frontier between areas 17 and 18a (dashed line), the potentials have nearly disappeared. Negative field potentials of increasing amplitude are observed anew for larger separations within area 18a and lead to the appearance of a large drop-shaped area. The antidromic action potential observed at 1.9 mm produces a stack of narrow rings.

Figure 2 illustrates the same kind of experiment for ‘feedback’ connections. A Nissl-stained section of the slice used for that experiment appears in Fig. 2A and a schematic representation of the same slice in Fig. 2B. The stimulating electrode, indicated by the cross, was located in the supragranular layers of area 18a. The different recording positions are represented by the dots in areas 18a and 17. They were separated from each other by 100 μm along the medio-lateral axis. The recordings were always obtained at 200 μm from the pial surface. This corresponds to the distance at which preliminary experiments showed large amplitude for ‘feedback’ field potentials.

Figure 2C shows the series of field potentials obtained for these different recording positions. Contrary to that of Fig. 1C, the series starts at the top of Fig. 2C with the recordings obtained at the largest distance from the stimulating electrode (3.38 mm) and ends with the smallest (0.88 mm). The recording obtained at the largest separation is flat. Then, as the electrode is displaced within area 17 towards area 18a, slow negative potentials appear and grow in amplitude until a separation of 2.78 mm, where the maximum amplitude is reached. Then the amplitude decreases until the potentials become flat (2.08 mm). All these slow negative potentials, indicative of synaptic activation, were obtained within area 17. Their onset latency was longer than 6 ms. They reach their maximum amplitude 3–5 ms after the onset. Compared with those of Fig. 1C, these potentials have a smaller amplitude, and reach the baseline faster. They were often preceded by fast negative potentials corresponding to antidromic action potentials (at 3.08, 2.68, 2.48 and 2.38 mm).

Traces obtained at 1.88–1.38 mm separations display a positive component only. These are likely to correspond to current sources. However, their latency and time course do not correspond to the negative potentials recorded in area 17. They are more likely to match the current sinks generated in area 18a, nearer the stimulating electrode. The following traces, from 1.28 to 0.88 mm, present more complex shapes. All have an early positive component, on which action potentials are sometimes superimposed, followed by a negative one.

Field potentials are plotted in a space-time domain in Fig. 2D. The presentation is inverted with respect to that of Fig. 2C, so that the upper part of the map corresponds to the intrinsic activity generated within area 18a. Between 0 and 3 ms, one can see a grey strip extending from the top to the base of the map, which corresponds to the stimulation artefact. Within area 18a, the potentials always begin with a positive component that has a latency of about 3 ms. The positive potentials are followed by negative potentials. These are less and less prominent as the distance from the stimulating electrode increases, and are finally replaced by potentials that are positive only. As the recording progresses in area 17, a

Fig. 2A–D Modification of field potential shape and amplitude for increasing horizontal separations and its relationship to the border between cortical areas 17 and 18a in a ‘feedback’ experiment. **A** Photomicrograph of a Nissl-stained section of the slice used for that experiment. The border between areas 17 and 18a is indicated by the *black arrow* and the alcian blue labels used as landmarks by the *open arrows*. **B** Schematic drawing of the same slice. The scale is not corrected for shrinkage. Conventions are as in Fig. 1B. **C** Series of potentials at decremental horizontal separations (indicated on the *right*). **D** *Upper part* Field potentials of **C** after resampling. *Lower part* Plot of field potentials in the space-time domain. The *grey areas* represent negative potentials and the *blank areas* positive potentials. Two regions of negative potential are visible: one in area 18a and another in area 17. They are separated by a region of positive potential near the border between areas 17 and 18a


A

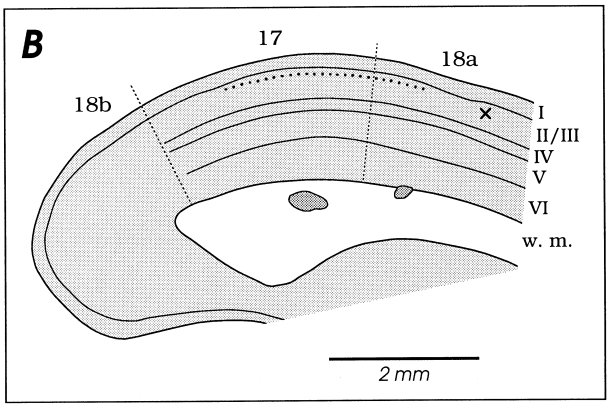
B
17
18a
18b
I
II/III
IV
V
VI
w. m.
2 mm

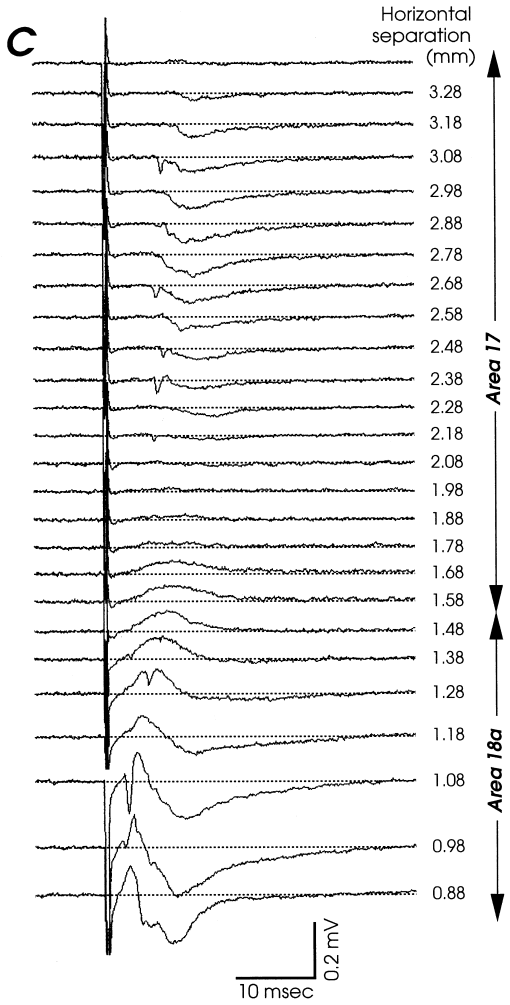
C
Horizontal separation (mm)
3.28
3.18
3.08
2.98
2.88
2.78
2.68
2.58
2.48
2.38
2.28
2.18
2.08
1.98
1.88
1.78
1.68
1.58
1.48
1.38
1.28
1.18
1.08
0.98
0.88
Area 17
Area 18a
0.2 mV
10 msec

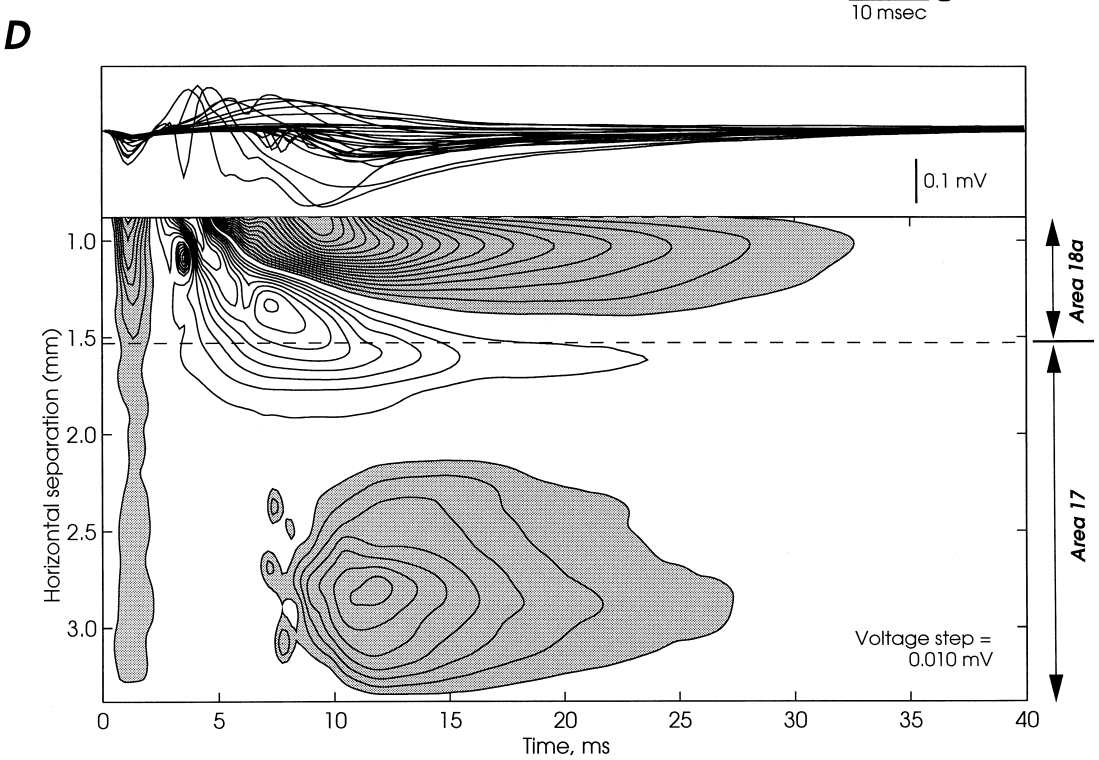
D
0.1 mV
Horizontal separation (mm)
1.0
1.5
2.0
2.5
3.0
Area 18a
Area 17
Voltage step =
0.010 mV
0
5
10
15
20
25
30
35
40
Time, ms

drop-shaped region of negative potential appears. It is preceded by action potentials that give rise to the small rings with latency around 7–8 ms.

Provided recordings were made in the supragranular layers, the features of the field potentials obtained at incremental horizontal separations from the stimulating electrode were similar for all experiments. The potentials obtained nearest the stimulating electrode displayed variable shapes and multiple components. Their amplitude was larger than that obtained in the other cortical area and their onset latency was always short, although precise measurements were not always possible due to the presence of the stimulation artefact.

As the recording site moved away from the stimulating electrode, field potentials decreased in amplitude, and finally reversed in sign. Positive potentials were either prominent, as in Fig. 2, or of small amplitude, as in Fig. 1, but were always observed. These positive potentials, which were always obtained in the vicinity of the border between the two cortical areas, indicated that the recording electrode was leaving the region in which activation was mediated by the intrinsic connections.

After this region of positive potentials, negative potentials were observed anew. Their shape was highly reproducible between experiments. Their onset latency was longer than that obtained with intrinsic activation (at these larger separations, the stimulation artefact was less prominent, allowing accurate measurements of latency). With respect to the onset latency, the peak latency was delayed by 5–8 ms. They returned to the baseline level in a slow and monotonic fashion.

Extensive mappings, such as those presented in Figs. 1 and 2, have been done in six cases for ‘feedforward’ and two cases for ‘feedback’ connections. The width of the region in which the field potentials displayed an amplitude equal to half the maximum amplitude (width at half height) was 690 and 630 μm for the ‘feedback’ experiments and averaged 424 ± 49 μm for the ‘feedforward’ experiments. This suggests stimulation in area 18a activated synapses over a larger surface of area 17, rather than the opposite. This is compatible with the larger size of area 17 compared with that of the different subfields of area 18a.

The distance from the stimulating electrode at which ‘feedforward’ field potentials displayed their maximum amplitude ranged between 1.5 and 3.3 mm (mean 2.2 mm). It was 1.9 mm and 2.6 mm for the two ‘feedback’ experiments. The maximum amplitude of the corticocortical field potentials and the distance from the stimulating electrode did not appear to be correlated.

These experiments indicate that intact corticocortical connections can be preserved in slices over long distances, and that interconnected loci can be located by electrophysiological means. Detailed (and time-consuming) mappings, such as those presented in Figs 1 and 2, were not done in all cases. However, less detailed mapping was done in all cases, since this is the method on which we relied to determine interconnected regions of areas 17 and 18a.

Mapping experiments were not always successful, but, provided a sufficient number of attempts with different stimulation sites were done, connected regions of area 17 and 18a could be identified in about 70% of the experiments.

Stimulation intensity

The relationship between stimulation intensity and field potentials amplitude is illustrated in Fig. 3. Figure 3A and C show the series of field potentials obtained at different stimulation intensities, for a ‘feedforward’ (Fig. 3A) and a ‘feedback’ (Fig. 3C) experiment. Figure 3B represents the relationship between stimulation intensity and the amplitude of the slow field potential of Fig. 3A measured at 13 and 20 ms (dashed vertical lines). Figure 3D presents the same relationship for the slow potential of Fig. 3C, measured at 11 and 14 ms (dashed vertical lines). In both cases, the amplitude first increases steeply, then more slowly, until it reaches a plateau. Fast potentials corresponding to orthodromic population spikes (arrow in Fig. 3A) appear when the stimulation intensity is larger than 40–50 μA. However, like the slow potentials, the fast potentials do not grow further with increasing stimulation intensity. This suggests the presence of a saturation phenomenon: the number of axons activated may increase as the stimulation current increases, until all axons that project near the recording site have been activated. The plateau of the field potential amplitude may also be related to the anodal surround phenomenon (that is, when axons are not activated but inhibited by large stimulation current: see Ranck 1975). The saturation could also correspond to the recruitment of inhibitory synapses that may shunt part of the late excitatory currents responsible for the negative potentials.

Increasing stimulation strength results in the appearance of orthodromic action potentials, but does not increase the amplitude of the slow synaptic potentials. Since we were mostly interested in synaptic responses, an intensity of 50 μA was used for field potential experiments – a compromise giving robust synaptic field potentials, with relatively little contamination by orthodromic action potentials.

Nature of synaptic potentials underlying the field potentials

In one ‘feedforward’ experiment, kynurenate (a broad antagonist of excitatory amino acids) was applied while recording field potentials (not shown). The kynurenate completely suppressed the slow field potentials.

Intracellular recordings of relatively large synaptic potentials were performed in ten cases, both in ‘feedforward’ and ‘feedback’ experiments. With small to moderate stimulation intensities, all the postsynaptic potentials (PSPs) that were depolarising at rest remained so when the neurones were depolarised by current injection, indi-

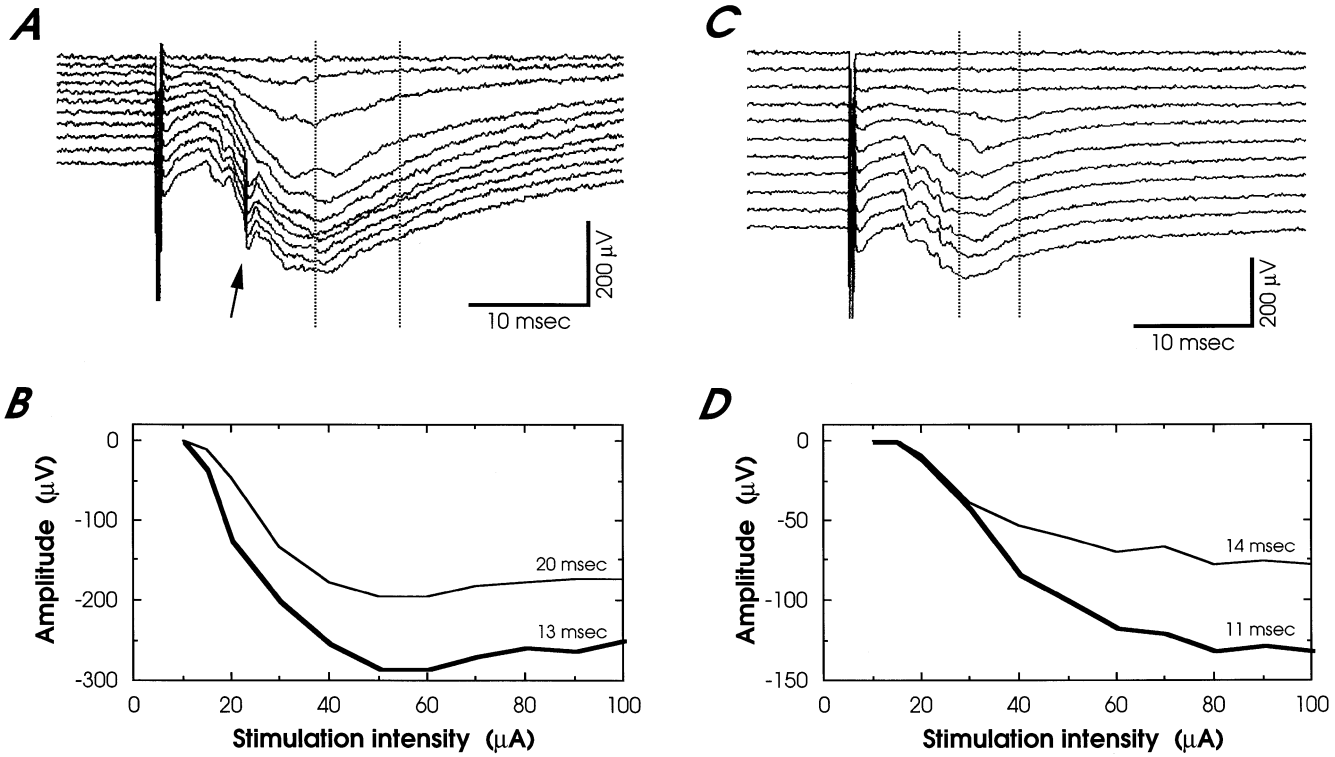

Fig. 3A–D Relationship between stimulation intensity and corticocortical field potential amplitude. **A, C** Series of potentials obtained at incremental stimulation intensities, for stimulation in area 17 and recording in area 18a (**A**), and for stimulation in area 18a and recording in area 17 (**C**). The first trace was obtained with a stimulation intensity of 10 µA, the second of 15 µA, the next one of 20 µA. Then the stimulating current was increased in steps of 10 µA up to 100 µA. **B** Relationship between stimulation intensity and field potential amplitude of the series shown in **A**. Amplitude was measured at 13 and 20 ms (*dashed vertical lines* in **A**). **D** Relationship between stimulation intensity and field potential amplitude of the series shown in **C**. Amplitude was measured at 11 and 14 ms (*dashed vertical lines* in **C**)

cating that these PSPs were excitatory and therefore likely to be mediated by excitatory amino acids.

The same experiments allowed us to examine their voltage dependency. An example is shown in Fig. 4A. This EPSP can be subdivided into two components: The early one displays a conventional voltage dependency, in that its amplitude was slightly reduced when the cell was depolarised. The late component displays an anomalous voltage dependency: it was not visible at rest but grew in amplitude when the cell was depolarised. Similar behaviour was observed in the majority of cases, for both 'feedforward' and 'feedback' EPSPs. It suggests that both Alpha-amino-3-hydroxy-5-methyl-4 isoxazole propionic acid (AMPA) AMPA and *N*-methyl-D-aspartate (NMDA) receptors may contribute to the EPSPs recorded (Thomson 1986; Artola and Singer 1990), although voltage-dependent conductances may also be involved in their anomalous voltage dependency (Stafstrom et al. 1985; Deisz et al. 1991; Hwa and Avoli 1992). In two cases, however, the whole of the EPSP decreased in amplitude with depolarisation of the neurone.

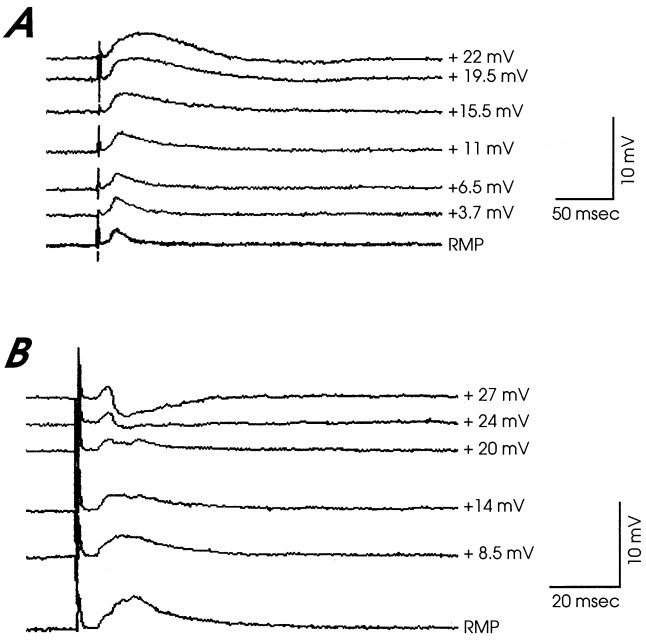

Fig. 4A, B Intracellular records of synaptic potentials. Synaptic potentials in **A** and **B** were recorded in area 17 after stimulation in area 18a. In **A** the stimulation intensity was 50 µA. Resting membrane potential (*RMP*) = –77 mV. When the cell was depolarised by intracellular current injection, the late part of the excitatory postsynaptic potential (EPSP) grew in amplitude while the earliest part showed little change. A series of recordings at different membrane potentials from another cell appears in **B**. The stimulation intensity was 100 µA in that case. At rest, the synaptic response is depolarising. This response consisted in an early EPSP, which remained depolarising 27 mV above rest, and an inhibitory postsynaptic potential (IPSP), which became hyperpolarising when the cell was sufficiently depolarised. *RMP* = –83 mV

Another question of interest is whether inhibitory postsynaptic potentials (IPSPs) contributed to the field potentials. It is usually assumed that IPSPs generate positive field potentials in vivo. However, the situation in vitro, where neurones have a resting membrane potential more negative than that in vivo, is somewhat different: IPSPs are *depolarising* at rest (Connors et al. 1982, 1988; Avoli and Olivier 1989) and would produce *negative* field potentials (inward current). The example of Fig. 4B shows that, in our experimental situation, IPSPs could indeed be depolarising at rest. At rest, the response to electrical stimulation consisted in a large depolarisation that corresponded in fact largely to an IPSP, revealed as such by depolarising the cell. This indicates that IPSPs could contribute to the negative potentials observed in our experiments. However, different lines of evidence (see Discussion) suggest that this contribution, at least to the earliest part of the field potentials, must be minor.

Laminar pattern of field potentials and current source density: 'feedforward' connections

In the majority of the experiments, stimulation was applied in the supragranular and infragranular layers in an interleaved fashion, such that recordings were obtained from the same groups of neurones for the two stimulation sites. The recordings were made 100 μm apart in the plane perpendicular to the cortical layers (referred to as 'depth'), starting at the top of cortex and ending near the border between white and grey matter or in the white matter. The laminar analysis was made for the position that yielded the largest field potentials during the horizontal mapping experiments such as those described in Fig. 1.

Results for a first 'feedforward' case are presented in Fig. 5. Figure 5A–C correspond to stimulation in the supragranular layers of area 17, Figs. D–F to stimulation in the infragranular layers.

The first traces of Fig. 5A, obtained at the surface of the cortex and within layer 1, appear positive. These positive potentials are indicative of current source. All the traces that were obtained deeper, from 0.2 up to 1.2 mm depth, are negative. The trace at 0.3 mm depth contains an antidromic action potential.

The spatio-temporal pattern of the field potentials shown in Fig. 5A is illustrated as a contour map in Fig. 5B. The largest negative potentials were obtained in layer 4. The contour map shows a second peak above the middle of the supragranular layers. Another region of negative potential can be seen in layer 5.

The corresponding CSD analysis is shown as a contour map in Fig. 5C. The areas shaded in grey correspond to current sinks, those left blank to current sources. Considering only the slowest components, one can see two regions of current sink: one is located in the upper half of the supragranular layers, the other is in layer 4 with a small extension to the bottom of layer 3. Three regions of current source are visible: one is in layer 1, and is likely to be associated with the current sink of the upper part of the supragranular layers. The two other current sources flank the layer 4 current sink in the supragranular layers and in layer 5. Therefore, the active synapses responsible for the field potentials of Fig. 5A and B were mainly located in the upper half of the supragranular layers and in layer 4.

Figure 5D–F present data obtained from the same experiment but with infragranular layer stimulation. The features of the potentials obtained at the different cortical depths are similar to those obtained with supragranular layer stimulation. Positive potentials are present in layer 1 and in the bottom of layer 6. The potentials obtained in all the other layers are negative. The slow field potentials are often preceded by sharp negative potentials corresponding to antidromic or orthodromic action potentials. The amplitude of the potential generated in the infragranular layers appears larger than that after supragranular layer stimulation, and provides an additional large peak in the lower half of layer 5 (Fig. 5E).

The CSD map of Fig. 5F shows the corresponding current sinks and sources. The antidromic and orthodromic action potentials generated groups of small rings at short latencies in all layers, and at long latencies in layer 5. Slow and long-lasting current sinks due to synaptic activation are present, as in Fig. 5C, in the upper half of the supragranular layers and in layer 4. However, an additional current sink, not present with supragranular layer stimulation, emerges just above the border between layers 5 and 6.

Another example of a laminar pattern of field potentials and associated CSD obtained in area 18a after stimulation in area 17 is illustrated in Fig. 6. The upper part (Fig. 6A–C) corresponds to supragranular layer stimulation in area 17, the lower part (Fig.6 D–F) to infragranular layer stimulation.

Examining the series of potentials of Fig. 6A shows little difference with that of Fig. 5A: Field potentials are positive in layer 1. They are negative for the remaining depths up to 1 mm. Then, traces present a shallow positivity until the white matter is reached. The trace obtained at 0.8 mm (in layer 5) is again contaminated by orthodromic action potentials from a bursting neurone. Examining the field potential contour map of Fig. 6B reveals one difference with respect to that of Fig. 5B that was not clearly visible on the series of potentials: the amplitudes of the field potentials have only a single maximum, located near the middle of the supragranular layers.

The CSD map of Fig. 6C further shows the presence of only one current sink, which extends from the upper third to the top of the supragranular layers. The current source associated with this sink occupies layer 1 and spreads slightly below the border between layers 1 and 2. The small current sources and sinks located in layer 5 result not from synaptic activities, but from the orthodromic action potentials of the layer 5 bursting neurone. Thus, the major difference between this case and the one depicted in Fig. 5 is that synaptic activation did not occur

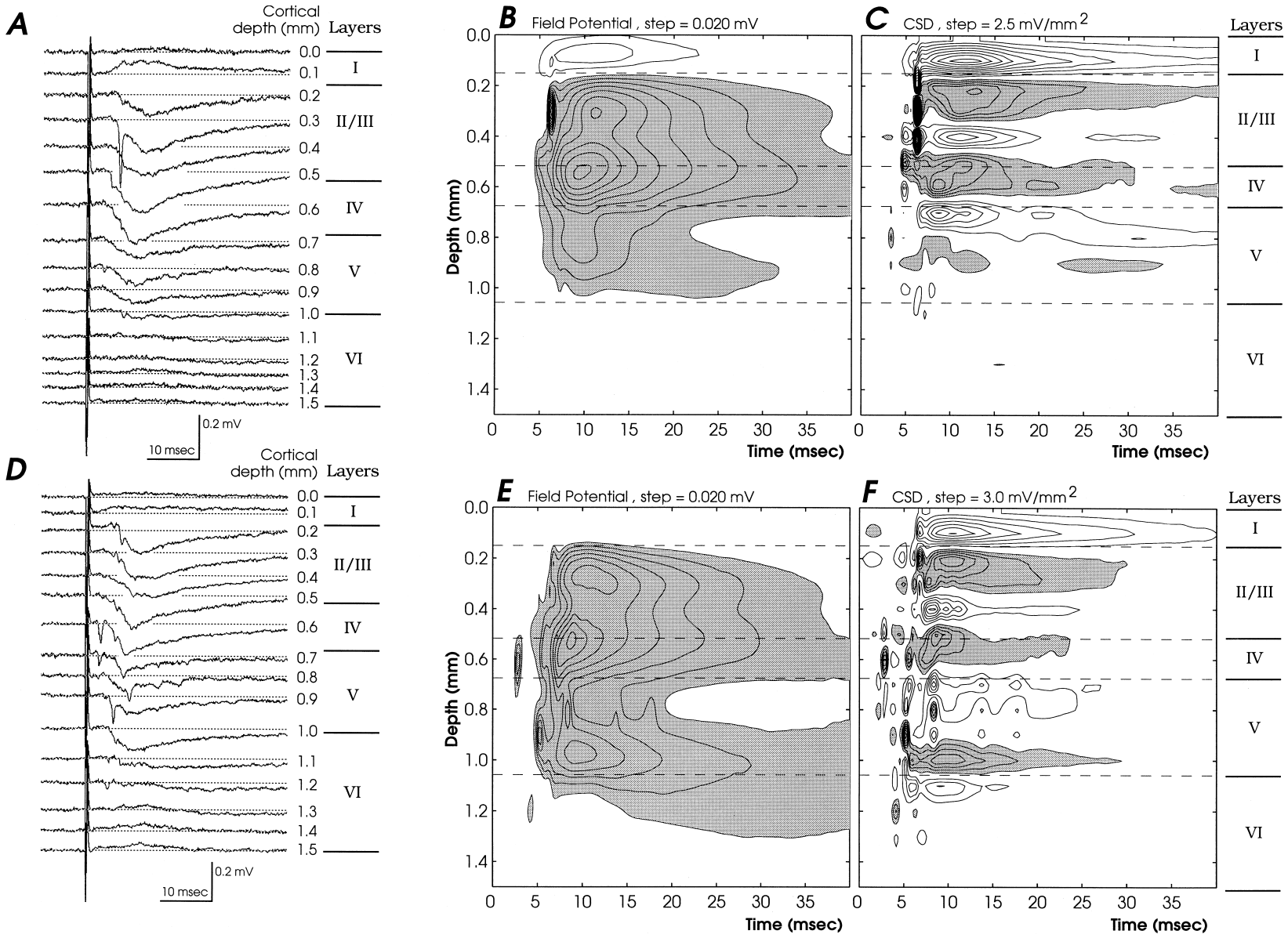

Fig. 5A–F Laminar pattern of field potentials and current source density (CSD) in a 'feedforward' experiment. Recordings were obtained in area 18a while stimulation was applied in area 17. The horizontal separation between both (supragranular and infragranular) stimulating electrodes and the recording sites was 1.95 mm. **A** Series of field potentials at different depths in area 18a, with stimulation in supragranular layers of area 17. Depths and cortical layers are indicated on the *right* of traces. **B** Field potentials plotted in the space-time domain. **C** Current source density map of the potentials appearing in **A** and **B**. **D–F** Same conventions as **A–C**, for stimulation in the infragranular layers of area 17

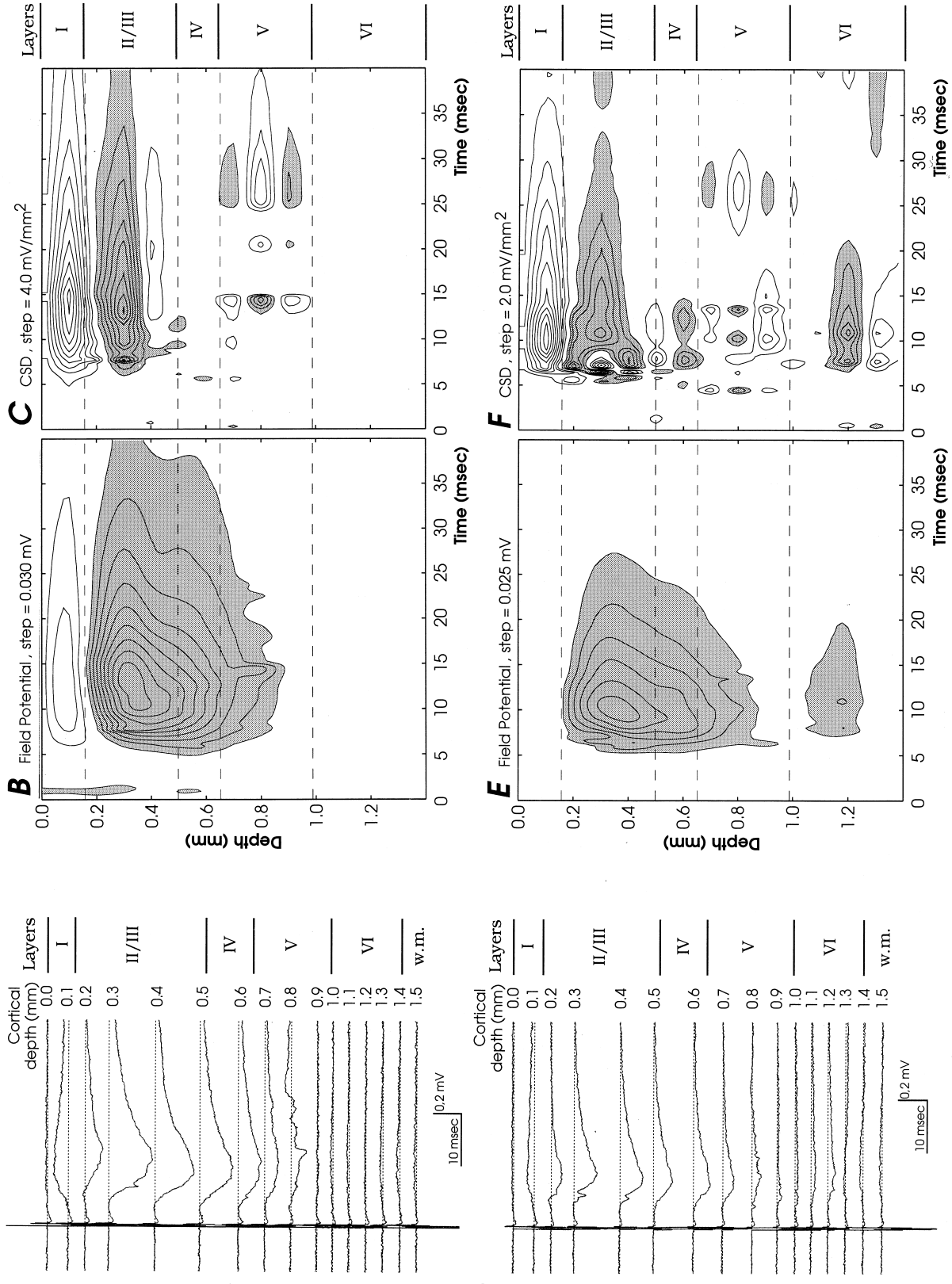

Fig. 6A–F Laminar pattern of field potentials and CSD in another 'feedforward' experiment. **A–C** Correspond to stimulation in the supragranular layers of area 17, and **D–F** to stimulation in the infragranular layers. Same conventions as in Fig. 5. The horizontal separations between the recording sites and the stimulating electrodes were 1.9 mm for supragranular stimulation and 1.85 mm for infragranular stimulation (the horizontal separation between the two stimulating electrodes and the recording axis was not always the same, due to curvature of the cortex)

in layer 4; it remained confined to the upper part of the supragranular layers.

The laminar organisation of the field potentials resulting from infragranular layer stimulation is shown in Fig. 6D and E. The shape and latency of the potentials are very similar to those obtained with supragranular layer stimulation. Nevertheless, two differences are visible: First the amplitude of the potentials recorded in the supragranular layers is smaller than that obtained after stimulation of the supragranular layers of area 17. Second, negative potentials appear in layer 6. Their amplitudes, however, are small compared with those of the supragranular layer potentials.

The CSD contour plot (Fig. 6F) differs to some extent from the one obtained after supragranular layer stimulation. The major current sink is still present in the supragranular layers, but its shape at the earliest latencies shows a bifurcation due to the action potentials observed at 0.3 and 0.4 mm. A current sink that was not observed after supragranular layer stimulation appears in the middle of layer 6. Finally, infragranular layer stimulation led to the appearance of a current sink in the bottom of layer 4. However, its amplitude is very small compared with that of the supragranular layers.

The laminar patterns of ‘feedforward’ field potentials and associated CSDs have been examined in six cases with supragranular layer stimulation in area 17 and four cases with stimulation in the infragranular layers. Because feedforward connections are thought to terminate predominantly in layer 4, we ranked the cases with respect to the strength of the current sink generated in layer 4. The example of Fig. 6C showed the presence of a current sink restricted to the upper part of the supragranular layers with no sink in layer 4. In a second case, the supragranular layer current sink was found to be wider than the one presented in Fig. 6, but no current sink appeared in layer 4. In a third case, the supragranular layer current sink was even wider, with its lowest part crossing the border between the supragranular layers and layer 4. In the fourth case, the single band of synaptic current sink described so far was replaced by two bands, the deeper of the two covering the upper part of layer 4 and the lowest part of the supragranular layers. In the fifth case, two bands of synaptic current were visible, as in the case of Fig. 5C, but the layer 4 current sink was slightly smaller than that of the supragranular layers. The final step in this ranking is represented by the case illustrated in figure 5C, where the supragranular and the layer 4 current sinks have comparable intensities.

These results indicate that the most consistent observation is the current sink in the upper part of the supragranular layers, with its associated current source in layer 1. Contrary to what could be expected given the anatomy of corticocortical connections, a current sink in layer 4 was not observed in all cases. Possible reasons for such a variability will be proposed in the Discussion. Finally, current sinks in the infragranular layers, when present after supragranular layer stimulation, were of negligible strength compared with those observed in the supragranular layers.

The same variability was observed in the four cases with stimulation in the infragranular layers of area 17: they always showed a current sink in the upper part of layer 2–3 and its associated current source in layer 1, but displayed variability with respect to the synaptic current sink in layer 4. In addition, infragranular layer stimulation led in all cases to the appearance of an additional large current sink in the infragranular layers that was not visible after supragranular stimulation. However, the position of this additional current sink was also variable from one experiment to another: it was observed in the lower half of layer 5 (Fig. 5F), or in the upper or middle part of layer 6 (Fig. 6F). The exact position of the infragranular current sink did not appear to be related to the pattern of synaptic activation in the supragranular layers and in layer 4.

When compared within one experiment, the current sinks generated in the supragranular layers and in layer 4 with supragranular layer stimulation were also observed with infragranular layer stimulation. In general, the amplitudes of the field potentials generated after stimulation of the infragranular layers were smaller than those obtained after stimulation of the supragranular layers.

Laminar pattern of field potentials and current source density: ‘feedback’ connections

In an attempt to characterise the responses generated by ‘feedback’ connections, we next examined the laminar organisation of functional synaptic inputs obtained after stimulation in area 18a and recording in area 17. Laminar mappings have been carried out in three experiments. In all cases stimulation was applied in both the supragranular and infragranular layers of area 18a. Results from two experiments are shown in Figs. 7 and 8.

Figures 7A and B illustrate the potentials obtained in area 17 at different depths when electrical stimulation was applied in the supragranular layers of area 18a. Negative potentials are observed in layer 1. This is different from experiments on ‘feedforward’ connections where the potentials in layer 1 were always positive. Negative potentials are also present in the supragranular layers. The largest is observed in the upper part of the supragranular layers just below layer 1 (0.2 mm depth). Smaller-amplitude slow potentials are also present in layer 5 and 4. The onset latency of the slow negative potentials is longer than 6 ms. Action potentials from a bursting neurone appear in the upper part of layer 5.

The associated CSD map is depicted in Fig. 7C. Numerous small rings are present, related to the action potentials visible in Fig. 7A. Considering only the slow events, one current sink can be observed covering layer 1 and the upper part of the supragranular layers.

Figure 7D–F illustrate data obtained during the same experiment but with electrical stimulation applied in the infragranular layers of area 18a. The field potential con-

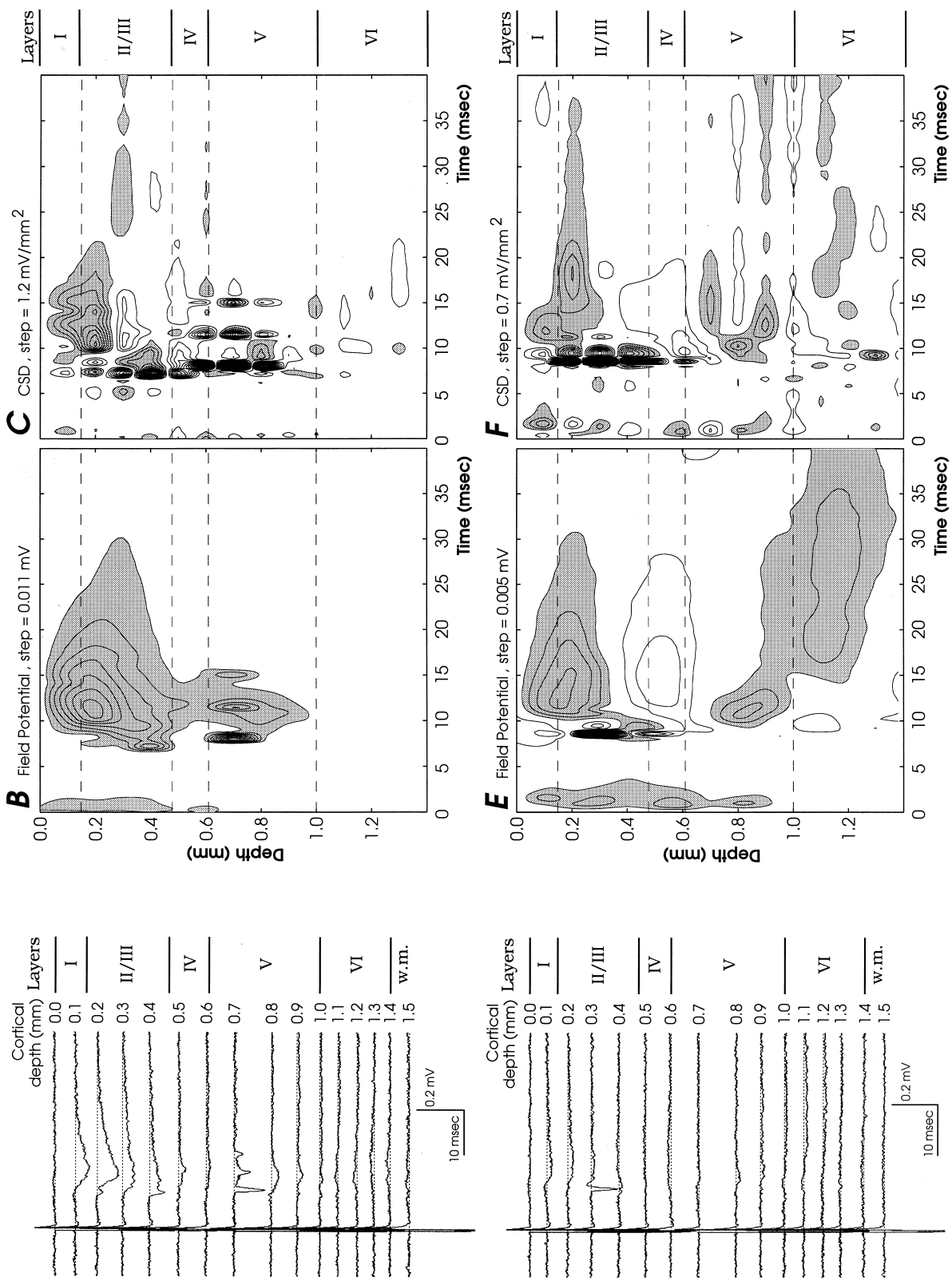

Fig. 7A–F Laminar pattern of field potentials and CSD in a 'feedback' experiment. Stimulation was in area 18a, recordings in area 17. The horizontal separations between the stimulating electrodes and the recording sites were 3 mm (supragranular electrode) and 2.7 mm (infragranular electrode). Conventions are the same as in Figs. 5 and 6. **A–C** Supragranular layer stimulation. **D–F** Infragranular layer stimulation. The amplitudes of the potentials in **D–F** are smaller than in Fig. 7A. The steps of the contour plot of Fig. 7E had to be adjusted in consequence. This results in the appearance of a grey line at post-stimulus times shorter than 5 ms in **E** and of current sink and sources in **F**, due to the stimulation artefact

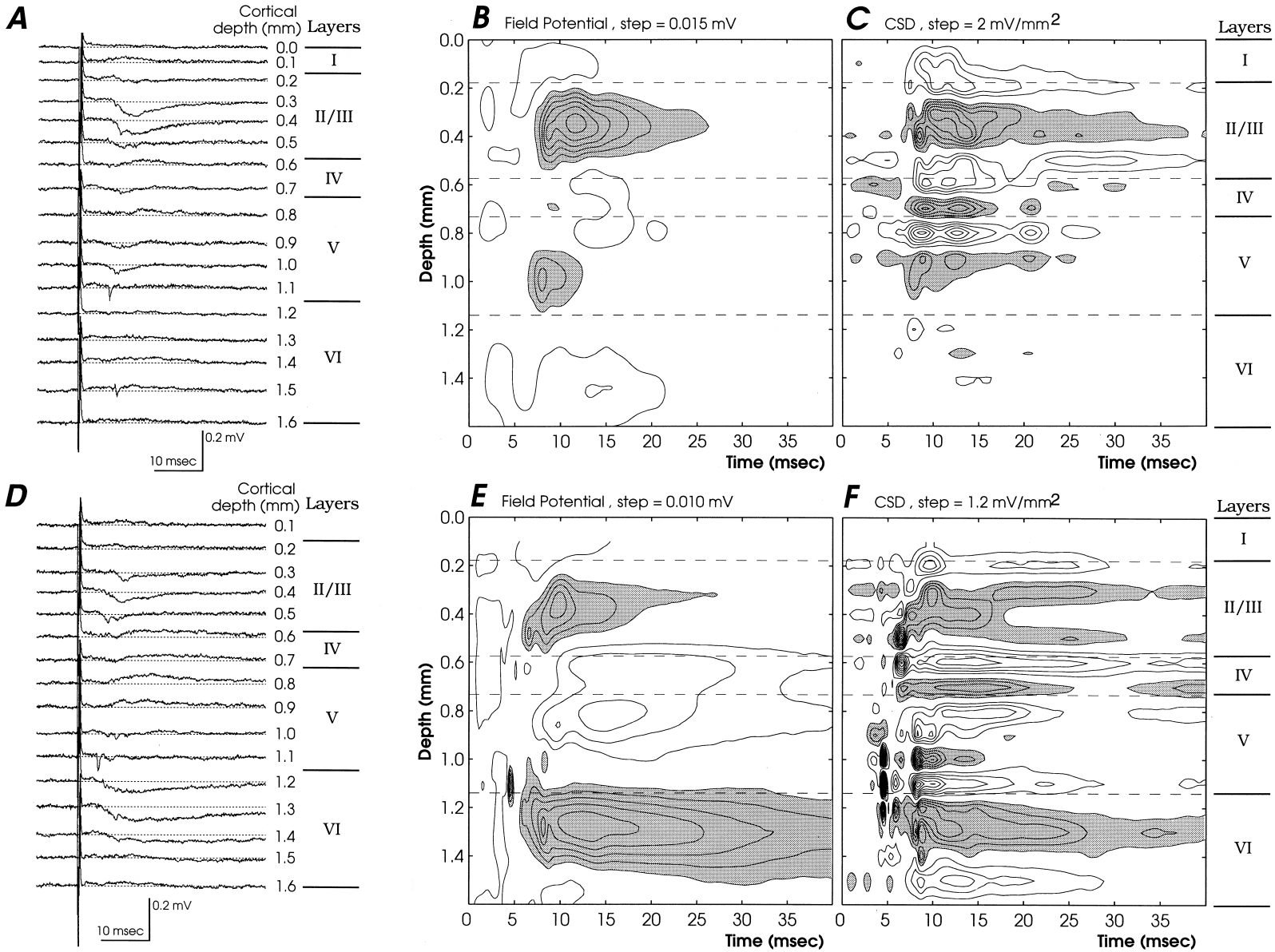

Fig. 8A–F Laminar pattern of field potentials and CSD in another 'feedback' experiment. Same conventions as in preceding figures. Recordings in area 17. **A–C** Supragranular layer stimulation in area 18a. **D–F** Infragranular layer stimulation in area 18a. First trace (0 mm depth) is missing. The horizontal separations between stimulating and recording electrodes were 1.9 mm (supragranular stimulation) and 1.7 mm (infragranular stimulation)

tour plot shows, as with supragranular layer stimulation, a region of negative slow potentials that includes layer 1 and the upper part of the supragranular layers. In addition, long-latency negative potentials are observed in layers 5 and 6.

Submitted to the CSD analysis (Fig. 7F), this series of field potential retains features essentially similar to those illustrated in Fig. 7C: The antidromic action potential observed at 0.3 mm depth generates the multiple ring-shaped sources and sinks in layers 2–3. A slow current sink of synaptic origin covers layers 1 and 2 between 10 and 15 ms after the stimulation, but disappears from layer 1 and remains in the upper half of the supragranular layers at post-stimulus time longer than 15 ms. The small negative potentials observed in the infragranular layers produce some regions of current sink, but their amplitudes are hardly higher than the noise level in layer 6.

Figure 8 illustrates the results of a second experiment on 'feedback' connections. In Fig. 8A the field potential recorded in layer 1 (0.1 mm depth) is positive, contrary to the one recorded in layer 1 of the preceding case. Negative field potentials, with onset latencies longer than 6.5 ms, are present in the middle of the supragranular layers (Fig. 8A, B). Negative potentials, of smaller amplitude but shorter latency, also appear in layer 5. Finally, small positive potentials are visible in layer 6.

The CSD map (Fig. 8C) demonstrates the presence of a large current sink in the upper half of the supragranular layers. It is accompanied by a current source that covers layer 1 and the top of the supragranular layers. Unexpectedly, another current sink of lower strength appears in the bottom of layer 4. It is separated from the first sink by a region of current source. Finally, a small sink appears in the middle of layer 5.

Figure 8D–F illustrate the pattern of activity obtained for the same experiment but with infragranular layer stimulation. Negative field potentials are still present in the supragranular layers. Although their amplitudes are smaller than those of potentials obtained after stimulation of the supragranular layers, their onset latencies appear shorter (4–6 ms). Infragranular layer stimulation resulted in the presence of additional negative potentials in layer 6 that have a larger amplitude and longer duration than those present in the supragranular layers. The CSD map (Fig. 8F) shows current sinks and sources comparable to those of Fig. 8C in the upper half of the cortex: a region of current sink is present in the supragranular layers, as well as a narrow strip extending along the bottom of layer 4. However, in the lower half of the cortex, infragranular layer stimulation resulted in the generation of a robust current sink in the upper part of layer 6, which was not observed after stimulation of the supragranular layers.

The third case studied in this series of 'feedback' experiments demonstrated the activation of synapses in the upper third of the supragranular layers, with a small extension in layer 1, for stimulation applied in both supra- and infragranular layers. However, most of layer 1 was occupied by a large current source. In both cases, a small current sink was visible in layer 5. Infragranular layer stimulation resulted in the appearance of an additional synaptic activation over the border of layers 5 and 6.

Thus, the results obtained for 'feedback' experiments also showed a variability in the pattern of synaptic activation. The strongest current sink was observed either in layer 1–2 or in the upper half of the supragranular layers. Similarly to what was observed for 'feedforward' experiments, stimulation in the infragranular layers of area 18a led to synaptic activation in the infragranular layers of area 17.

One difference was obvious between 'feedforward' and 'feedback' experiments, namely the potentials obtained after stimulation of area 18a were smaller than those obtained after stimulation of area 17. The mean amplitude of the largest potentials obtained for 'feedforward' experiments was –177.7 ± 27.4 mV (n = 10, supra- and infragranular layer stimulation combined) compared with –65.6 ± 9.4 mV for 'feedback' experiments (n = 6, supra- and infragranular layer stimulation combined). The difference is significant (P = 0.0034).

Latency

Latency measurements have been made for several events. First, we recorded intracellularly 15 monosynaptic *unitary EPSPs* (uEPSPs), i. e. EPSPs that resulted from the activation of a single axon. These EPSPs were all evoked by stimulation applied in area 17 while recordings were performed in area 18a. Two examples are presented in Fig. 9A and B (note the different time scales for A and B). Their unitary nature was recognised by their small amplitude and their occurrence in an all-or-nothing fashion. They were monosynaptic as determined by their short and constant latency, their fast rise time, and their ability to sustain high-frequency stimulation (up to 20 Hz). The threshold to evoke them ranged between 1 and 12 μA (mean 6.3 μA). Their mean amplitude was 0.896 ± 0.110 mV (range 0.189–1.840 mV), which places them in the upper range of uEPSPs determined for intrinsic connections by spike-triggered averaging (Komatsu et al. 1988; Thomson et al. 1988*)*, dual intracellular recording (Mason et al. 1991; Nicoll and Blakemore 1993; Thomson and West 1993; Thomson et al. 1993) and minimal electrical stimulation (Volgushev et al. 1995). It is possible, however, that this relatively large mean amplitude resulted from a sampling bias towards the largest EPSPs. Their rise time was 2.014 ± 0.351 ms and their width at half height was 5.727 ± 0.914 ms.

The distribution of their latency is presented in Fig. 9C. The mean latency was 6.967 ± 0.389 ms. The histogram further shows a relatively wide range of latency for the uEPSPs (4.4–9.4 ms).

The onset latency of *field potentials* elicited in 'feedforward' and 'feedback' experiments is presented in Fig. 9D. The onset latency of 'feedforward' field potentials was 4.96 ± 0.34 ms. That of 'feedback' potentials was between 6.7 and 7.8 ms. This apparent difference is

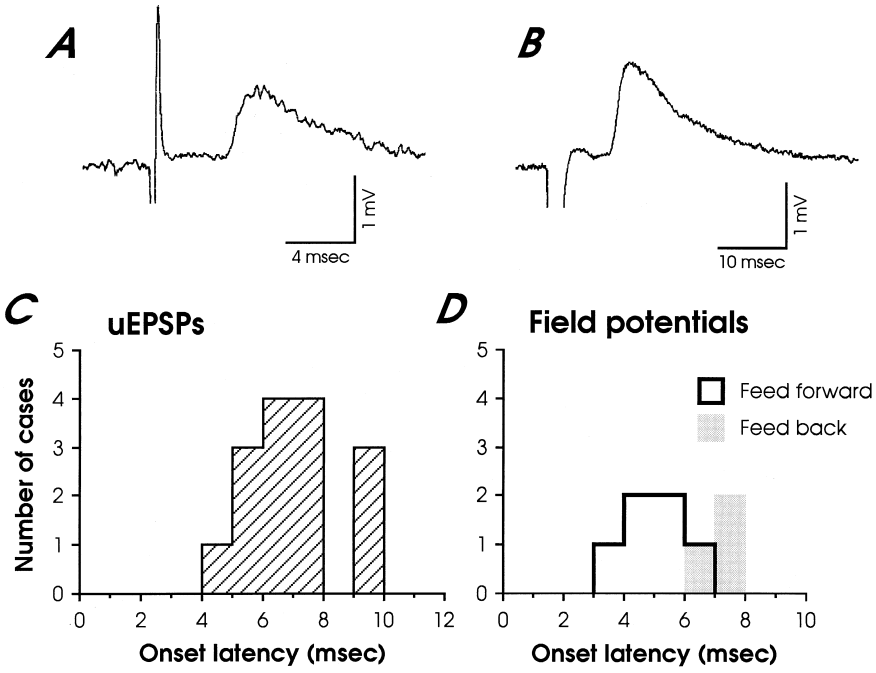

Fig. 9A–D Latency of unitary EPSPs and field potentials. **A**, **B** Two examples of unitary EPSPs (note different time scales). Traces are averages over 50 repetitions. **C** Histogram representing the distribution of the onset latency of unitary EPSPs. **D** Histogram of the onset latency of field potentials. Only laminar profiles obtained with supragranular layer stimulation have been considered

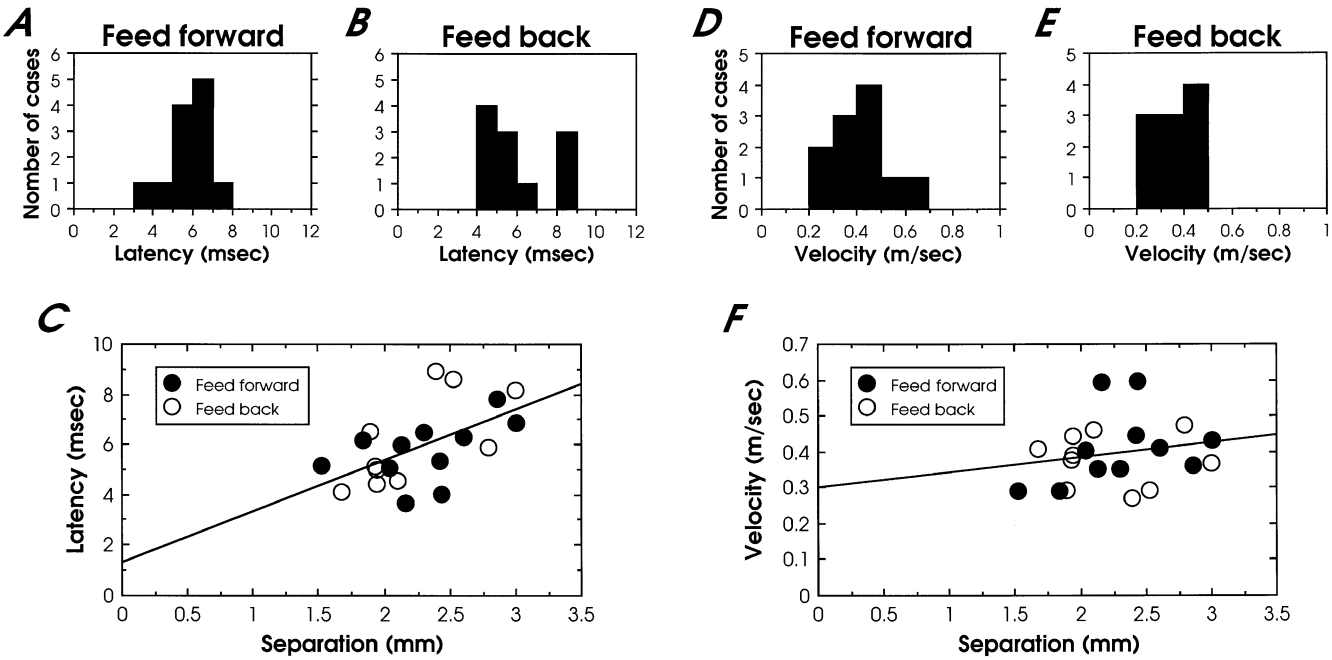

Fig. 10A–F Latency for antidromic activation of corticocortical neurones and conduction velocity of their axons. **A** Distribution of antidromic latency for neurones involved in feedforward connections (stimulation in area 18a, recordings in area 17). **B** Distribution of antidromic latency for neurones involved in feedback connections (stimulation in area 17, recordings in area 18a). **C** Relationship between antidromic latency and separation between stimulating and recording electrodes. The sample size is smaller than in **A** and **B** due to missing values of separation for one feedforward and one feedback case. The equation of the regression line is: Latency (ms) = 2.025 × separation (mm) + 1.352 (r^2 = 0.323, where r is the correlation coefficient). The histogram in **D** represents the distribution of conduction velocity of the axon of neurones involved in feedforward connections, that in **E** of the axon of neurones involved in feedback connections. **F** Conduction velocity represented as a function of separation between recording and stimulating electrode. There is no significant relationship in that case (r^2 = 0.04)

in fact related to different distances between recording and stimulating sites. When velocities were compared to take the distance into account, no difference was observed between ‘feedforward’ and ‘feedback’ field potentials.

When compared with that of the uEPSPs, the onset latency of ‘feedforward’ field potentials was significantly *shorter* (P = 0.005). This can be understood since the latency of the field potentials is determined by that of the fastest axons. In that respect, the shortest latencies for uEPSPs and field potentials differed by 0.5 ms only (3.9 and 4.4 ms, respectively).

The temporal aspects of responses produced through corticocortical pathways was further studied using measurement of latencies for *antidromic action potentials*.

For the reasons already mentioned (see Materials and methods), we concentrated on data obtained after stimulation of the supragranular layers of area 17 or area 18a. Some of the antidromically activated neurones were identified during field potential experiments. Others have been recorded with tungsten-in-glass microelectrodes. Two have been intracellularly recorded and identified as regularly spiking neurones. The antidromic latencies are presented in the histograms of Fig. 10A and B. The mean latency for neurones involved in 'feedforward' connections was 5.69 ± 0.34 ms (range 3.66–7.87 ms, $n = 12$); that for neurones of 'feedback' connections was 6.00 ± 0.54 ms (range 4.1–8.9 ms, $n = 11$). The distributions of latencies for the two populations do not differ ($P = 0.97$).

The graph of Fig. 10C illustrates the relationship between antidromic latency and separation between recording and stimulating electrode. The slope of the regression line is significantly different from 0 ($P = 0.007$, *t*-test on slope), indicating that the onset latency increases as a function of the separation.

Figure 10D and E present the distributions of conduction velocities. The velocity of axons involved in 'feedforward' connections (0.413 ± 0.31 m/s, range 0.291–0.6 m/s) and that of axons involved in 'feedback' connections (0.377 ± 0.023 m/s, range 0.270–0.476 m/s) do not differ significantly ($P = 0.72$). These data also indicate some dispersion of conduction velocities, with the slowest axons having conduction velocities that are half those of the fastest.

The relationship between conduction velocity and separation between recording and stimulating electrode is depicted in Fig. 10F. Contrary to what was observed for latency, there is no significant relationship ($P = 0.3$, *t*-test on slope).

Discussion

Localisation of corticocortical connections in vitro

The aim of our experiments was to study the synaptic physiology of corticocortical connections in vitro. The first step was to establish their preservation despite the slicing procedure. Area 18a contains a number of functional visual areas (Montero 1973, 1993; Montero et al. 1973a, b; Olavarria and Montero 1981,1984; Cusick and Lund 1981; Thomas and Espinoza 1987; Coogan and Burkhalter 1993; Orbach and Van Essen 1993). Some of these areas establish reciprocal connections with area 17 that are oriented parallel to the frontal plane (Montero et al. 1973b; Olavarria and Montero 1981; Coogan and Burkhalter 1993; Montero 1993), which is the plane used for slicing. The terminal field observed in area 18a after anterograde labelling of forward connections appears relatively narrow: 300–400 μm diameter in Montero et al. (1973b), about 500 μm diameter in Coogan and Burkhalter (1993). Therefore, it seemed possible that at least part of these connections could remain intact in 500 μm thick slices. By mapping of the field potentials along the medio-lateral axis, we indeed found interconnected regions in area 17 and 18a in the majority of our experiments, with separation between the stimulating electrode and the largest corticocortical potential of between 1.5 and 3.3 mm.

The shape of the field potentials varied as the recordings were obtained farther and farther away from the stimulating electrode (Figs. 1, 2). Field potentials generated through intrinsic connections displayed complex shapes and large amplitudes. As the recording progressed away from the stimulating electrode, their amplitude decreased. This decrease must be related to the reduction in density of terminals from intrinsic axon collaterals, which in labelling experiments do not spread farther than 1–1.5 mm from the injection site (Burkhalter 1989; Burkhalter and Charles 1990; Lohmann and Rörig 1994). Orbach and Van Essen (1993) showed that electrical activation of intrinsic horizontal collaterals in rat area 17 leads to synaptic activation in a radius of about 1 mm around the stimulating electrode.

Further away from the region in which intrinsic negative potentials were observed, positive potentials were recorded that are likely to correspond to current sources accompanying current sinks generated by the activation of intrinsic connections. These positive potentials were useful electrophysiological landmarks that indicated the recording micropipette was leaving the region of intrinsically generated field potentials.

With continued progression away from the stimulating electrode, one of two things happened: either the potentials remained flat, and it was concluded that the stimulation failed to activate the corticocortical connections, or the recording micropipette entered a region where negative potentials reappeared and grew in amplitude with increasing separation from the stimulating electrode. This distant region of negative potentials was always in a cortical area different from the one in which electrical stimulation was applied, as shown by histological examination. Within area 18a, the nearest functional subdivision that lies medial to area 17 is the area called 'LM' (Montero et al. 1973b; Montero 1981). The recordings for 'feedforward' experiments were presumably obtained in this area. The stimulation, for 'feedback' experiments, was presumably applied in LM too.

Interconnected loci were not observed with separation *smaller* than 1.5 mm for the largest amplitude. Two reasons may account for this observation: (1) For small separations there may be a continuity of negative potentials, from the intrinsic to the extrinsic corticocortical connections, without the clear transition we relied on to ascertain we were entering another cortical area. (2) Alternatively, the large positive potentials generated after intrinsic activation may have obscured the negative potentials associated with corticocortical connections with small separations. This points to the fact that the separation between stimulating and recording electrodes must be large enough for an unambiguous electrophysiological identification of interconnected loci.

Contrary to those elicited through intrinsic connections, the corticocortical field potentials recorded in the supragranular layers had a stereotyped and reproducible shape: their rise time was long, usually around 5 ms, and their decay was slow and monotonic. The 'feedforward' field potentials differed from the 'feedback' field potentials not by their shape, but by their larger amplitude.

From pharmacological manipulation or from intracellular recordings, we inferred that the earliest part of the field potentials corresponded to monosynaptic excitatory potentials. This confirms the results obtained by Johnston and Burkhalter (1994) who showed that neurones of both feedforward and feedback connections are retrogradely labelled by tritiated aspartate captured by their terminals.

Although inhibitory synapses can generate current sinks (Fig. 4), a number of arguments suggest that their contribution to the field potentials is very small. First, EPSPs were evoked in isolation with moderate stimulation intensities (50 μA in Fig. 4A); higher intensities were required to generate IPSPs (100 μA in Fig. 4B). Second, the onset latency of the IPSPs was delayed by 3–5 ms with respect to the onset of the EPSPs. These two observations suggest that the IPSPs were disynaptic. Third, orthodromic action potentials were only rarely encountered with the stimulation strength used (50 μA). Therefore, the contribution of disynaptic responses to the field potentials must have been minimal and, if significant, must have been limited to their latest part. Further arguments have been presented in support of the preponderance of excitatory currents in field potentials (Mitzdorf 1985).

In a recent study, McDonald and Burkhalter (1993) suggested that direct inhibitory connections link area 17 and 18a. In our intracellular recordings we never observed IPSPs in isolation. IPSPs were visible only with stimulation intensity stronger than that producing isolated EPSPs, and their latency was longer. Both features are consistent with these IPSPs being disynaptically generated. It suggests that, if a direct inhibitory linkage exists between area 17 and 18a, it must contribute a fairly small number of synapses compared with the direct excitatory linkage.

Laminar pattern of field potential and current source density analysis

The second step in our study was to study the functional anatomy of corticocortical connections. For that purpose, we used extracellular recording of field potentials and their analysis by CSD.

The proper application of the one-dimensional CSD analysis requires that the current flows in only one of the three spatial dimensions. For corticocortical field potentials, positive potentials, indicating current sources, were observed only along the depth axis. They were not observed in the horizontal dimension (Figs. 1, 2). They were also not observed when recordings were made at different depths below the surface of the slice (not illustrated). This suggests that most the of current was flowing in one dimension, that of the depth axis.

The data we obtained after CSD analysis showed a pronounced variability. Electrical stimulation in area 17 was expected to reveal synaptic activation in layer 4 of area 18a, but this was observed in only half the cases. Stimulation in area 18a was expected to reveal a synaptic activation in layer 1 of area 17, but this occurred in only one third of the cases. The possibility that this could be explained by the fact that some slices were damaged by the preparation appears unlikely because, in all cases, the potentials were stable during several hours of recordings and there was no relationship between the type of CSD pattern and the sizes of the potentials (with the exception of the smaller size of the 'feedback' potentials observed in all cases).

The most likely explanation for this variability is related to the use of electrical stimulation. In another paper (Nowak and Bullier 1997a) it has been shown that electrical stimulation does not activate cell bodies, but axons. It follows that the stimulation applied, for example in area 17, activated the efferent axons of area 17, those that are involved in feedforward connections, but it also activated axonal trunks and terminals of the afferents to area 17, including axons involved in feedback connections. The antidromic action potentials propagating backwards along the main axon could have invaded the intrinsic recurrent axon collaterals. This invasion could have resulted in an orthodromic activation in area 18a.

Given that antidromic responses have been observed in only two of 21 intracellularly recorded cells, one may argue that the activation of the recurrent collaterals does not account for a large part of the recorded signal. However, after stimulation of an axon, the antidromic invasion may be observed in only one cell body but invasion of the collaterals can produce an orthodromic response in, say, 100 other cells. This means that the invasion of axon collaterals could account for *all* the recorded signal.

Therefore, the field potentials presented in this paper may have resulted from the activation of two pathways: one is the 'real' corticocortical pathway; the other corresponds to an intrinsic collateral pathway *specific* to the neurones from which corticocortical axons are issued. The variability reported in our experiments could be related to the relative weight of these two pathways in the stimulated axons. This could vary in different experiments because of variability in the cutting process. Another possible explanation is given below.

One important difference between these two sets of axons is the size of their terminal arbors. As schematised in Fig. 11, feedforward axons arborize in area 18a over a region smaller than 0.5 mm in the horizontal dimension (Montero et al. 1973b; Coogan and Burkhalter 1993). On the other hand, the intrinsic collaterals from supragranular layer neurones arborise over more than 1 mm (Lohmann and Rörig 1994). The laminar pattern of synaptic activity generated by stimulation in area 17 will then de-

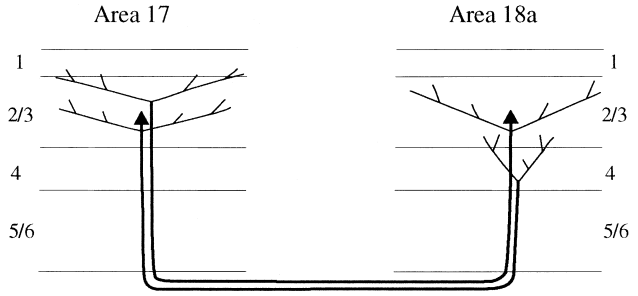

Fig. 11 Horizontal extent of intrinsic and corticocortical axonal arborisations in areas 17 and 18a. The smaller extent of the terminal arborisations of feedforward axons compared with that of collaterals of feedback axons may explain why current sinks are not always observed in layer 4, whereas current sinks are always observed in upper layers 2–3 in area 18a after stimulation in area 17 ('feedforward' experiments). A similar reasoning could explain the variability in laminar distribution of current sinks and sources for 'feedback' experiments (see text)

pend on the precise placement of the *recording* electrode in area 18a (Fig. 11). If it is placed exactly within the region where the activated feedforward axons arborise, then both pathways will contribute to the field potentials. If the recording electrode is displaced laterally with respect to the focus of feedforward connection terminals, then it is possible that only the intrinsic collaterals will contribute to the field potentials. At intermediate positions, variable importance of the synaptic contribution of either pathway may be the basis for differences in strengths of activation in the different cortical layers.

In all the 'feedforward' experiments, a strong synaptic activation occurred in the upper part of the supragranular layers that was accompanied by a prominent current source in layer 1. We attribute this to the activation of intrinsic axon collaterals in area 18a. It implies that neurones that are sending feedback axons have intrinsic collaterals providing the bulk of their functional synapses to the upper part of the supragranular layers. This is consistent with labelling studies showing intrinsic anterograde tracing mostly in the upper part of supragranular layers of visual cortical areas in the rat (Coogan and Burkhalter 1993). The CSD study of Luhmann et al. (1990) performed in cat area 17 also showed that the stimulation of intrinsic horizontal connections leads to a strong synaptic activation of the upper part of the supragranular layers.

In a subset of our 'feedforward' experiments we observed a strong activation in layer 4 and the bottom of layer 3. We hypothesise that this resulted from recording in the arborisation region of the 'real' feedforward axons. This strong and focussed synaptic response is in keeping with the conclusion of Olavarria and Montero (1981) that feedforward axons terminate mostly in layer 4, but is at odds with other reports (see introduction) that indicate that layer 4 is not the major site of termination of feedforward connections in the rat.

Variability in CSD patterns was also observed for 'feedback' experiments. This could again be related to the difference in arborisation patterns of intrinsic collaterals and feedforward axons in area 18a. Because of the restricted terminal arbors of feedforward axons, antidromic activation of intrinsic collaterals of feedforward neurons in area 17 is not always present. This is consistent with the observation in one case of a restricted activation of layer 1 and the upper part of layers 2–3 (Fig. 7), which is likely to correspond to a specific activation of the feedback pathway. The CSD pattern obtained in that case is very similar to the one obtained by Cauller and Connors (1994) after stimulation of the isolated layer 1. It could mean that the feedback connections provide their strongest synaptic inputs to the very top of the cortex.

In the two other cases of feedback connections studied, the main synaptic activation was observed in the upper part of the supragranular layers, and was accompanied by a current source in layer 1. This pattern of activity might reflect the activation of intrinsic collaterals.

In all the cases of 'feedforward' and 'feedback' experiments, although in variable amount, infragranular layer stimulation led to the appearance of a synaptic activation in the infragranular layers that was not observed with supragranular layer stimulation. This pattern is consistent with the anatomical results showing a segregation of pathways from supra- and infragranular layers (Henry et al. 1991; Coogan and Burkhalter 1993). However, one cannot rule out the participation of intrinsic collaterals. Corticocortical neurones that provide axonal arborisation in the infragranular layers of their target area may also have intrinsic collaterals in the infragranular layers.

In summary, the CSD patterns suggest the presence of a synaptic activation in the upper part of the supragranular layers by the intrinsic collaterals of neurones involved in corticocortical connections. The strongest feedforward inputs would target the upper half of layer 4 and the lowest part of layer 3. Feedback connections would generate the bulk of their synaptic activation in layer 1 and the upper part of the supragranular layers. In addition, infragranular layer neurones would be the recipients of synaptic inputs from either the infragranular layers of the other cortical area, or their own intrinsic collaterals.

These conclusions are similar to those reached in a recent study by Domineci et al. (1995), which also reports CSD analyses of the synaptic responses elicited by feedforward and feedback connections in rat visual cortex. Variability is also apparent in the results reported by this group, since two of their illustrations (Figs. 4, 5) do not show a current source in layer 4 after a 'feedforward' stimulation.

Response latency

The conduction velocity of the axons involved in area 17–18a connections ranges between about 0.25 m/s and 0.6 m/s. The field potential latency may be used to estimate the velocity of the fastest axons, which appears to

be less than 0.8 m/s. These values have been calculated assuming that the axons follow a straight course between the stimulating and the recording electrode. Since the course of some axons is likely to be U-shaped, a correction should be applied. Given the width of rat cortex (1 mm) and the interelectrode distance (2 mm), a correction factor of 2 is a reasonable estimate, giving conduction velocities between 0.5 and 1.2 m/s. This indicates that the axons involved in rat corticocortical connections are very slowly conducting, as in a number of other species (Nowak and Bullier 1997b; Bullier et al 1988; Swadlow and Weyand 1981). This slow conduction of corticocortical axons contrasts with the situation for many peripheral axons. For comparison, the conduction velocities of rat retinal ganglion cells are larger than 1.7 m/s and can be as fast as 24 m/s (Hale et al. 1979).

Since there is a relationship between conduction velocity and axonal diameter (Rushton 1951; Waxman and Bennett 1972; Nowak and Bullier 1997b), we can extrapolate that the diameters of the stimulated axons were between 0.07 and 0.17 μm. According to Waxman and Bennett (1972), 0.2 μm is the lowest limit below which myelination does not increase conduction velocity. Therefore, it is to be expected that corticocortical axons in rat visual cortex are mainly small-diameter unmyelinated axons.

We found a significant relationship between the latency of antidromic activation and the distance separating recording and stimulating electrodes (Fig. 10C), but no correlation could be observed between axonal conduction velocity and separation (Fig. 10F). This suggests that there is no compensation for increased distance by increased conduction velocities for corticocortical connections. This is at variance with what has been observed in other brain structures, such as the cerebellum where the longest olivocerebellar fibres have higher conduction velocities than the shorter fibres (Sugihara et al. 1993).

Our conclusion that feedforward and feedback connections have similar conduction velocities is similar to that reached in the monkey visual cortex by comparing the diameters of feedforward and feedback axons between areas V1 and V2 (Rockland and Virga 1989 1990). This suggests that feedback axons are involved in the transmission of information across cortical areas (Nowak and Bullier 1997b), instead of playing a slow modulatory role as is usually assumed.

Acknowledgements We thank Pascale Giroud and Naura Chounlamountri for help during the experiments, Pierre-Marie Chorrier for technical help, Christian Urquizar for help with the electronic and programming, and Veronique Chenavier for programming. This work was supported by H.F.S.P. no. RG 55/94. L.G.N. was supported by a grant from the Ministère de la Recherche et de la Technologie.

References

Artola A, Singer W (1990) The involvement of *N*-methyl-D-aspartate receptors in induction and maintenance of long-term potentiation in rat visual cortex. Eur J Neurosci 2: 254–269

Avoli M, Olivier A (1989) Electrophysiological properties and synaptic responses in the deep layers of human epileptogenic neocortex in vitro. J Neurophysiol 61: 589–605

Bullier J, McCourt ME, Henry GH (1988) Physiological studies on the feedback connection to the striate cortex from cortical areas 18 and 19 of the cat. Exp Brain Res 70: 90–98

Burkhalter A (1989) Intrinsic connections of rat primary visual cortex: laminar organization of axonal projections. J Comp Neurol 279: 171–186

Burkhalter A, Charles V (1990) Organization of local axon collaterals of efferent projection neurons in rat visual cortex. J Comp Neurol 302: 920–934

Cauller LJ, Connors BW (1994) Synaptic physiology of horizontal afferents to layer I in slices of rat SI neocortex. J Neurosci 14: 751–762

Connors BW, Gutnick MJ, Prince DA (1982) Electrophysiological properties of neocortical neurons in vitro. J Neurophysiol 48: 1302–1320

Connors BW, Malenka RC, Silva LR (1988) Two inhibitory postsynaptic potentials, and $GABA_A$ and $GABA_B$ receptor mediated responses in neocortex of rat and cat. J Physiol (Lond) 406: 443–468

Coogan TA, Burkhalter A (1988) Sequential development of connections between striate and extrastriate visual cortical areas in the rat. J Comp Neurol 278: 242–252

Coogan TA, Burkhalter A (1993) Hierarchical organization of areas in rat visual cortex. J Neurosci 13: 3749–3772

Cusick CG, Lund RD (1981) The distribution of the callosal projection to the occipital visual cortex in rats and mice. Brain Res 214: 239–259

Deisz RA, Fortin G, Zieglgänsberger W (1991) Voltage dependence of excitatory postsynaptic potentials of rat neocortical neurons. J Neurophysiol 65: 371–382

Dreher B, Shameen N, Thong IG, McCall MJ (1985) Development of cortical afferents and cortico-tectal efferents of the mammalian (rat) primary visual cortex. Aust N Z J Ophthalmol 13: 251–261

Domenici L, Harding GW, Burkhalter A (1995) Patterns of synaptic activity in forward and feedback pathways within rat visual cortex. J Neurophysiol 74: 2649–2664

Dürsteler MR, Blakemore C, Garey LJ (1979) Projections to the visual cortex in the golden hamster. J Comp Neurol 183: 185–204

Freeman JA, Nicholson C (1975) Experimental optimization of current source-density technique for anuran cerebellum. J Neurophysiol 38: 369–382

Haberly LB, Sheperd GM (1973) Current-density analysis of summed evoked potentials in opossum prepiriform cortex. J Neurophysiol 36: 789–802

Hale PT, Sefton AJ, Dreher B (1979) A correlation of receptive field properties with conduction velocity of cells in the rat's retino-geniculo-cortical pathway. Exp Brain Res 35: 425–442

Henry GH, Salin PA, Bullier J (1991) Projections from areas 18 and 19 to cat striate cortex: divergence and laminar specificity. Eur J Neurosci 3: 186–200

Hughes HC (1977) Anatomical and neurobehavioral investigations concerning the thalamo-cortical organization of rat's visual system. J Comp Neurol 175: 311–336

Hwa GG, Avoli M (1992) Excitatory postsynaptic potentials recorded from regular-spiking cells in layers II/III of rat sensorimotor cortex. J Neurophysiol 67: 728–737

Johnson RR, Burkhalter A (1992) Corticocortical feedback connections in visual cortex synapse selectively with dendritic spines. Soc Neurosci Abstr 18: 300

Johnson RR, Burkhalter A (1994) Evidence for excitatory amino acid neurotransmitters in the forward and feedback corticocortical pathways within rat visual cortex. Eur J Neurosci 6: 272–286

Kennedy H, Bullier J (1985) A double-labelling investigation of the afferent connectivity to cortical areas V1 and V2 of the macaque monkey. J Neurosci 5: 2815–2830

Komatsu Y, Nakajima S, Toyama K, Fetz EE (1988) Intracortical connectivity revealed by spike-triggered averaging in slice preparations of cat visual cortex. Brain Res 442: 359–362

Krieg WJS (1946a) Connections of the cerebral cortex. I. The albinos rat. A. Topography of the cortical areas. J Comp Neurol 84: 221–275

Krieg WJS (1946b) Connections of the cerebral cortex. I. The albinos rat. B. Structure of the cortical areas. J Comp Neurol 84: 277–323

Lohmann H, Rörig B (1994) Long-range horizontal connections between supragranular pyramidal cells in the extrastriate visual cortex of the rat. J Comp Neurol 344: 543–558

Luhmann HJ, Greuel JM, Singer W (1990) Horizontal interactions in cat striate cortex. II. A current source-density analysis. Eur J Neurosci 2: 358–368

Lund JS, Hendrickson AE, Ogren MP, Tobin TE (1981) Anatomical organization of primate visual cortex area VII. J Comp Neurol 202: 19–45

Mason A, Nicoll A, Stratford K (1991) Synaptic transmission between individual pyramidal neurons of the rat visual cortex in vitro. J Neurosci 11: 72–84

Maunsell JHR, Van Essen DC (1983) The connections of the middle temporal visual area (MT) and their relationship to a cortical hierarchy in the macaque monkey. J Neurosci 3: 2563–2586

McCormick DA, Connors BW, Lighthall JW, Prince DA (1985) Comparative electrophysiology of pyramidal and sparsely spiny stellate neurons of the neocortex. J Neurophysiol 54: 782–806

McDonald CT, Burkhalter A (1993) Organization of long-range inhibitory connections within rat visual cortex. J Neurosci 13: 768–781

Merrill EG, Ainsworth A (1972) Glass-coated platinum-plated tungsten microelectrodes. Med Biol Eng 10: 662–672

Miller MW, Vogt BA (1984) Direct connections of rat visual cortex with sensory, motor, and association cortices. J Comp Neurol 226: 184–202

Mitzdorf U (1985) Current source-density method and application in cat cerebral cortex: investigation of evoked potentials and EEG phenomena. Physiol Rev 65: 37–100

Mitzdorf U, Singer W (1978) Prominent excitatory pathways in the cat visual cortex (A 17 and A 18): a current source density analysis of electrically evoked potentials. Exp Brain Res 33: 371–394

Mitzdorf U, Singer W (1979) Excitatory synaptic ensemble properties in the visual cortex of the macaque monkey: a current source density analysis of electrically evoked potentials. J Comp Neurol 197: 71–84

Montero VM (1973) Evoked responses in the rat's visual cortex to controlateral, ipsilateral and restricted photic stimulation. Brain Res 53: 192–196

Montero VM (1981) Comparative studies on the visual cortex. In: Woolsey CN (ed) Cortical sensory organization, vol 2. Multiple visual areas. Humana Press, Clifton, NJ, pp 33–81

Montero VM (1993) Retinotopy of cortical connections between the striate cortex and extrastriate visual areas in the rat. Exp Brain Res 94: 1–15

Montero VM, Rojas A, Torrealba F (1973a) Retinotopic organisation of striate and peristriate visual cortex in the albinos rat. Brain Res 53: 197–201

Montero VM, Bravo H, Fernandez V (1973b) Striate-peristriate cortico-cortical connections in the albinos and gray rat. Brain Res 53: 202–207

Nicholson C, Freeman JA (1975) Theory of current source-density analysis and determination of conductivity tensor for anuran cerebellum. J Neurophysiol 38: 356–368

Nicoll A, Blakemore C (1993) Single-fibre EPSPs in layer 5 of rat visual cortex in vitro. Neuroreport 4: 167–170

Nowak LG, Bullier J (1996) Spread of stimulating current in cortical grey matter of rat visual cortex. J Neurosci Methods 67: 237–248

Nowak LG, Bullier J (1997a) Axons, but not cell bodies are activated by electrical stimulation in cortical gray matter. II. Evidence from selective inactivation of cell bodies and axon initial segments. Exp Brain Res (in press)

Nowak LG, Bullier J (1997b) The timing of information transfer in the visual system. In: Kaas, J, Rockland K, Peters A (eds) Extrastriate cortex. (Cerebral cortex, vol 12) (in press)

Olavarria J, Montero VM (1981) Reciprocal connections between the striate cortex and extrastriate cortical areas in the rat. Brain Res 217: 358–363

Olavarria J, Montero VM (1984) Relation of callosal and striate-extrastriate cortical connections in the rat: morphological definition of extrastriate areas. Exp Brain Res 54: 240–252

Orbach HS, Van Essen DC (1993) In vivo tracing of pathways and spatio-temporal activity patterns in rat visual cortex using voltage sensitive dyes. Exp Brain Res 94: 371–392

Ranck JB (1975) Which elements are excited in electrical stimulation of mammalian central nervous system? A review. Brain Res 98: 417–440

Ribac CE, Peters A (1975) An autoradiographic study of the projections from the lateral geniculate body of the rat. Brain Res 92: 341–368

Rockland KS, Pandya DN (1979) Laminar origins and terminations of cortical connections of the occipital lobe in the rhesus monkey. Brain Res 179: 3–20

Rockland KS, Virga A (1989) Terminal arbor of individual 'feedback' axons projecting from area V2 to V1 in the macaque monkey: a study using immunohistochemistry of anterogradely transported *Phaseolus vulgaris* leucoagglutinin. J Comp Neurol 285: 54–72

Rockland KS, Virga A (1990) Organization of individual cortical axons projecting from area V1 (area 17) to V2 (area 18) in the macaque monkey. Vis Neurosci 4: 11–28

Rockland KS, Saleem KS, Tanaka K (1994) Divergent feedback connections from areas V4 and TEO in the macaque. Vis Neurosci 11: 579–600

Rushton WAH (1951) A theory of the effects of fibre size in medullated nerve. J Physiol (Lond) 115: 101–122

Spatz WB, Vogt DM, Illing R-B (1991) Delineation of the striate cortex, and the striate-peristriate projections in the guinea pig. Exp Brain Res 84: 495–504

Stafstrom CE, Schwindt PC, Chubb MC, Crill WE (1985) Properties of persistent sodium conductance and calcium conductance of layer V neurons from cat sensorimotor cortex in vitro. J Neurophysiol 53: 153–170

Sugihara I, Lang EJ, Llinás R (1993) Uniform olivocerebellar conduction time underlies Purkinje cell complex spike synchronicity in the rat cerebellum. J Physiol (Lond) 470: 243–271

Swadlow HA, Weyand TH (1981) Efferent systems of the rabbit visual cortex: laminar distribution of cells of origin, axonal conduction velocities and identification of axonal branches. J Comp Neurol 203: 799–822

Thomas HC, Espinoza SG (1987) Relationship between interhemispheric cortical connections and visual areas in hooded rats. Brain Res 417: 214–224

Thomson AM (1986) A magnesium-sensitive post-synaptic potential in rat cerebral cortex resembles neuronal responses to *N*-methylaspartate. J Physiol (Lond) 370: 531–549

Thomson AM, West DC (1993) Fluctuation in pyramid-pyramid excitatory synaptic potentials modified by presynaptic firing pattern and postsynaptic membrane potential using paired intracellular recording in rat neocortex. Neuroscience 54: 329–346

Thomson AM, Gilderstone D, West DC (1988) Voltage-dependent currents prolong single-axon postsynaptic potentials in layer III pyramidal neurons in rat neocortical slices. J Neurophysiol 60: 1896–1907

Thomson AM, Deuchars J, West DC (1993) Large, deep layer pyramid-pyramid single axon EPSPs in slices of rat motor cortex display paired pulse and frequency-dependent depression, mediated presynaptically and self facilitation, mediated postsynaptically. J Neurophysiol 70: 2354–2369

Tigges J, Tigges M, Perachio AA (1977) Complementary laminar terminations of afferents to area 17 originating in area 18 and the lateral geniculate nucleus in squirrel monkey. J Comp Neurol 176: 87–100

Volgushev M, Voronin LL, Chistiakova M, Artola A, Singer W (1995) All-or-none excitatory postsynaptic potentials in the rat visual cortex. Eur J Neurosci 7: 1751–1760

Wabha G (1990) Spline models for observational data. CBMS-NSF. (Regional conference series in applied mathematics, vol 59). Society for Industrial and Applied Mathematics, Philadelphia

Waxman SG, Bennett MVL (1972) Relative conduction velocities of small myelinated and non-myelinated fibres in the central nervous system. Nature New Biol 238: 217–219

Waxman SG, Swadlow HA (1976) Ultrastructure of visual callosal axons in the rabbit. Exp Neurol 53: 115–127